Lithos 233 (2015) 89–110

Contents lists available at ScienceDirect

Lithos

journal homepage: www.elsevier.com/locate/lithos

Platinum-group element signatures in the North Atlantic Igneous Province: Implications for mantle controls on metal budgets during continental breakup

Hannah S.R. Hughes *, Iain McDonald, Andrew C. Kerr

School of Earth and Ocean Sciences, Cardiff University, Main Building, Cardiff CF10 3AT, United Kingdom

ARTICLE INFO

Article history:
Received 22 December 2014
Accepted 8 May 2015
Available online 16 May 2015

Keywords:
North Atlantic Igneous Province
British Palaeogene Igneous Province
Iceland plume
PGE
Lava

ABSTRACT

The North Atlantic Igneous Province (NAIP) is a large igneous province (LIP) that includes a series of lava suites erupted from the earliest manifestations of the (proto)-Icelandic plume, through continental rifting and ultimate ocean opening. The lavas of one of these sub-provinces, the British Palaeogene Igneous Province (BPIP), were some of the first lavas to be erupted in the NAIP and overlie a thick crustal basement and sedimentary succession with abundant S-rich mudrocks. We present the first platinum-group element (PGE) and Au analyses of BPIP flood basalts from the main lava fields of the Isle of Mull and Morvern and the Isle of Skye, in addition to a suite of shallow crustal dolerite volcanic plugs on Mull, and other minor lavas suites. BPIP lavas display both S-saturated and S-undersaturated trends which, coupled with elevated PGE abundances (>MORB), suggest that the BPIP is one of the most prospective areas of the NAIP to host Ni–Cu–PGE–(Au) mineralisation in conduit systems. Platinum-group element, Au and chalcophile element abundances in lavas from West and East Greenland, and Iceland, are directly comparable to BPIP lavas, but the relative abundances of Pt and Pd vary systematically between lavas suites of different ages. The oldest lavas (BPIP and West Greenland) have a broadly chondritic Pt/Pd ratio (~1.9). Lavas from East Greenland have a lower Pt/Pd ratio (~0.8) and the youngest lavas from Iceland have the lowest Pt/Pd ratio of the NAIP (~0.4). Hence, Pt/Pd ratio of otherwise equivalent flood basalt lavas varies temporally across the NAIP and appears to be coincident with the changing geodynamic environment of the (proto)-Icelandic plume through time. We assess the possible causes for such systematic Pt/Pd variation in light of mantle plume and lithospheric controls, and suggest that this reflects a change in the availability of lithospheric mantle Pt-rich sulphides for entrainment in ascending plume magmas. Hence the precious metal systematics and potential prospectivity of a LIP may be affected by contamination of plume-derived magmas by subcontinental lithospheric mantle at the margins of cratons that have been enriched by Palaeoproterozoic orogenesis.

1. Introduction

Some of the world's most important orthomagmatic Ni–Cu–PGE sulphide deposits reside in continental flood basalt provinces, or large igneous provinces (LIPs)—for example the Norilsk–Talnakh conduit-hosted mineralisation in the Siberian Traps (e.g., Arndt, 2011). Many factors contribute to the formation of such deposits, not the least the timing of S-saturation and segregation of immiscible sulphide liquids, triggered by various processes including contamination of magmas by crustal S-rich sediments (e.g., Ripley et al., 2003). Sulphur-saturation may also be achieved by magma mixing or fractional crystallisation of ascending magmas (e.g., Irvine, 1975; Naldrett, 2011 and references therein). Once formed, immiscible sulphide liquids scavenge chalcophile elements from repeated influxes of silicate magma, and if collected, may form sulphide deposits and mineralisation within intrusions such as mid- to upper-crustal magma conduits (e.g., Naldrett, 2004, 2011).

The North Atlantic Igneous Province (NAIP) is a LIP and certain portions are documented to host Au–Cu–PGE mineralisation, such as the Skaergaard Intrusion, Kap Edvard Holm Complex, and associated Macrodykes in East Greenland (Bird et al., 1991, 1995; Andersen et al., 1998; Arnason and Bird, 2000; Thomassen and Nielsen, 2006; Holwell et al., 2012). Continental flood basalts in West Greenland appear to have undergone assimilation-induced S-saturation, highlighted as potentially overlying significant orthomagmatic PGE mineralisation,

Abbreviations: NAIP, North Atlantic Igneous Province; BPIP, British Palaeogene Igneous Province; PGE, platinum-group elements; REE, rare earth elements; NAC, North Atlantic Craton; MSS, monosulphide solution; SDRS, Seaward Dipping Reflector Series; LIP, large igneous province.

* Corresponding author at: School of Geosciences, University of the Witwatersrand, PVT Bag 3, Wits 2050, Johannesburg, South Africa. Tel.: +27 11 717 6585.
E-mail address: hannah.hughes@wits.ac.za (H.S.R. Hughes).

http://dx.doi.org/10.1016/j.lithos.2015.05.005

and are currently under exploration (e.g., Keays and Lightfoot, 2007 and references therein). In contrast, onshore and offshore continental flood basalts in this region, along with basaltic lavas of the seaward dipping reflectors offshore of the Southeast Greenlandic coast, are predominantly S-undersaturated (Philipp et al., 2001; Momme et al., 2002). However, minor S-saturation has taken place in some flows here, following silicate magma differentiation and fractionation (Philipp et al., 2001).

Aside from S-saturation, the initial concentration of PGE, Ni and Cu in mantle-derived magmas is a key factor in the probability of their forming orthomagmatic mineralisation (e.g., Naldrett, 2004). Worldwide, such mineralisation appears to be correlated with the occurrence of mantle plume events impinging on thick cratonic (Archaean) lithospheric mantle (e.g., Groves and Bierlein, 2007; Maier and Groves, 2011 and references therein). The debate over the cause for this association remains unresolved (e.g., Arndt, 2013). This may imply some dependence on there being high-degree melting and/or deeper mantle (or even mantle–core) melting associated with mantle plumes, and hence important geochemical/geophysical constraints on mineralisation potential specific to plumes. Alternatively the association may suggest enrichment of PGE in cratonic subcontinental lithospheric mantle (SCLM) which could become incorporated in ascending LIP magmas. It may also reflect a biased preservation and/or discovery potential (e.g., Maier and Groves, 2011).

The magmatic centres and plateau lavas of the British Palaeogene Igneous Province (BPIP) formed prior to continental breakup and at a similar time to continental flood basalts in West Greenland (Storey et al., 2007 and references therein). However, no significant Ni–Cu–PGE exploration has taken place in the BPIP to date, despite favourable circumstances for crustal S contamination in this region (see Andersen et al., 2002). In this paper we report new platinum-group element (PGE) and Au analyses for a series of BPIP basaltic lavas to establish their S-saturation status, and to assess the fertility and prospectivity of the Eastern part of the BPIP.

PGE abundances in various Greenlandic and Icelandic lava suites will be compared with our new BPIP lava dataset in order to assess the implications for mineralisation potential and metal ratios, from early plume impingement beneath the continental lithosphere, throughout continental breakup and ultimately during oceanic rifting (± a non-plume mid-ocean ridge melting component).

2. Geology and formation of the North Atlantic Igneous Province (NAIP)

Impingement of the proto-Icelandic mantle plume under the continental lithosphere of Greenland, Canada and Europe (i.e., beneath the North Atlantic Craton; NAC) generated the NAIP. Prior to this, Greenland and Europe were joined and seafloor spreading had previously initiated in the South Labrador Sea between Canada and Greenland (ca. 80 Ma; Roest and Srivistava, 1989) during a period of slow extension apparently devoid of extensive volcanism (Chambers and Pringle, 2001). However, ca. 62 Ma, significant volumes of mafic magmatism below what is now the UK, Greenland and Baffin Island (Fig. 1), signified a dramatic change in thermal mantle conditions, which predated continental rifting (c. 55 Ma) but ultimately led to the opening of the Atlantic Ocean (Saunders et al., 1997). The main products of this prolonged period of magmatism were alkali and tholeiitic flood basalts. In total, Palaeocene and Eocene magmas of the NAIP likely ranged from 5 to 10×10^6 km^3 in volume (White and McKenzie, 1989; Holbrook et al., 2001 and references therein). The NAIP can be divided into several distinct igneous temporal intervals, as outlined below (Saunders et al., 1997; Chambers and Pringle, 2001; Jolley and Bell, 2002; Storey et al., 2007)—see Fig. 2.

Continent-based magmatism and stretching during impingement of the proto-Icelandic mantle plume (pre- and syn-breakup; ca. 62–56 Ma):

1 Phase 1—The onset of widespread and voluminous volcanism initially in West Greenland and Baffin Island at 61.7 ± 0.5 Ma (Sinton et al., 1998) comprising basaltic and picritic lavas up to ~7 km thick (Storey et al., 2007), and alkali basaltic lavas in the Faroe–Shetland Basin and Scottish (Hebridean) portion of the BPIP. At the end of this interval there was a switch to localised, and increasingly intermittent, volcanic activity (ca. 57–56 Ma).
2 Phase 2—Eruption of widespread volcanic sequences due to an increase in melt production rate at 56.1 ± 0.5 Ma which coincided with continental rifting (Storey et al., 2007). Tholeiitic basaltic sequences were erupted in West and East Greenland (e.g., Blosseville Kyst, Kangerlussuaq, and Hold with Hope regions), the Irmiger Basin, Faroe Islands, Vøring Plateau, Faroe–Shetland Basin, Rockall Basin, and the Inner Hebrides and Antrim (BPIP).

Syn- and post-breakup, plate separation at the Mid-Atlantic Ridge (56 Ma to present):

3 Phase 3—Voluminous volcanism continued, but was restricted to the margins of the proto-North Atlantic rift, forming abnormally thick oceanic crust offshore and along the line of plate separation, ca. 56–50 Ma (Philipp et al., 2001; Storey et al., 2007 and references therein). Basalts from this period are observed in the Irmiger Basin, Faroe Islands, East Greenland margin, and the Vøring Plateau and are seismically imaged as seaward-dipping reflector sequences.
4 Phase 4—Continuing volcanism of the Iceland plume diminished and narrowed along a restricted portion of the East Greenland margin along the Greenland–Iceland ridge (ca. 50 Ma) to present-day hotspot activity in Iceland (Storey et al., 2007).

The position of the (proto-) Icelandic mantle plume has moved through time relative to the overlying tectonic plates (Fig. 1—e.g., Lawver and Muller, 1994). The various methods used to assess the centre of the plume (e.g., locus of highly magnesian lavas) suggest that the Palaeogene proto-Icelandic plume lay beneath central Greenland in the Palaeogene and Early Eocene, and gradually tracked SE–ESE beneath what is now the Greenland–Iceland ridge (delineated as a zone of thickened oceanic crust) to its present day position beneath Iceland at the Mid-Atlantic Ridge.

2.1. The Hebridean portion of the BPIP

The BPIP is part of the earliest magmatic series of the NAIP, which includes Palaeogene rocks of the Hebridean Igneous Province (along the W coast of Scotland) and Northern Ireland (Fig. 3). In the Scottish Hebrides, the BPIP includes the Isles of Mull, Skye, the Small Isles, and the mainland igneous complex of Ardnamurchan and lava flows of Morvern. The crustal sequence into which the magmas of the Hebridean portion of the BPIP were intruded includes the Archaean basement rocks of the Lewisian Gneiss Complex (part of the NAC), Mesoproterozoic Stoer, Sleat and Torridon Group sediments (mostly coarse sandstones, with some shale and silt members), areas of Neoproterozoic Dalradian and Moine metasediments, Triassic limestones and a thick package (>1 km estimated total thickness) of Jurassic and minor Cretaceous sediments representing part of the Hebrides Basin (Fig. 3).

Emeleus and Bell (2005) provide a comprehensive compendium of radiometric and palynological age determinations from various published sources. Broadly, the eruption of lavas in this province spanned approximately 3 Myr (61–58 Ma; White and Lovell, 1997). Detailed work by Single and Jerram (2004) has revealed volcanic disconformities within eroded lava fields. Such juxtaposition of volcanic sites and lava batches of the same geochemical type, common in the Hebrides, is a feature of continental flood basalt plateaus which were fed by multiple centres or fissure systems, and must be taken into account in regional lava suite correlation (Jerram and Widdowson, 2005).

2.1.1. The Isle of Mull and Morvern lavas and doleritic plugs

The Mull lava succession (Fig. 3) is estimated as being 1800 m thick and covering approximately 840 km^2 (Emeleus and Bell, 2005); the maximum thickness presently exposed in a single section is 1000 m on Ben More (Kerr, 1995a). These flat-lying lavas overlie thin Upper

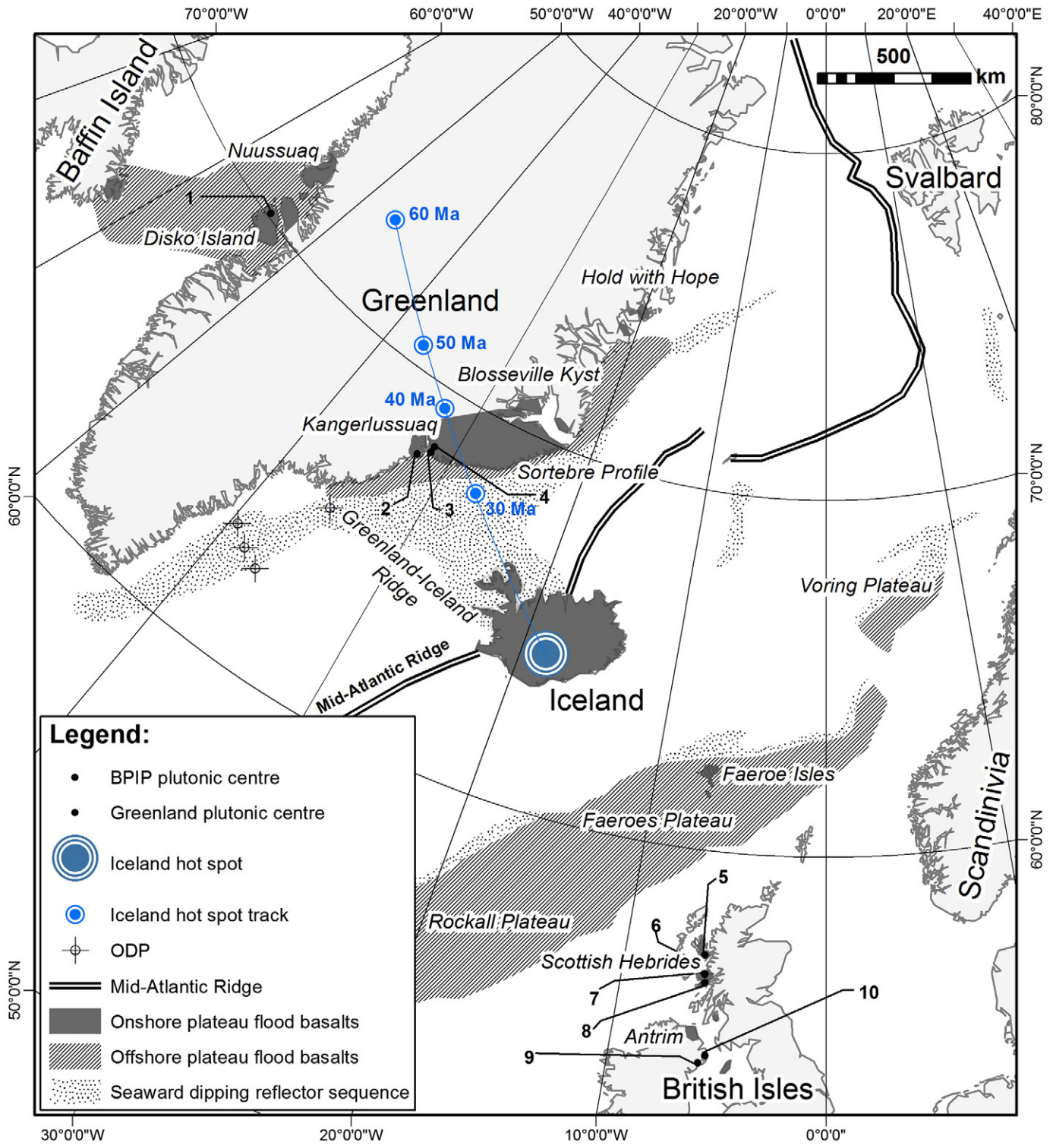

Fig. 1. Simplified Palaeogene geology of the NAIP, showing locations of the flood plateau basalts associated with early-stage rifting of the Atlantic and a selection of plutonic centres; (1) Hammer Dal Complex, Disko Island, (2) Krusse Fjord Complex, (3) Skaergaard Complex, (4) Miki Fjord and Togeda Macrodykes, (5) Cuillin Central Complex, Isle of Skye, (6) Rum Central Complex, Isle of Rum, (7) Central Complexes of Ardnamurchan, (8) Ben Buie Central Complex, Isle of Mull, (9) Carlingford Complex, and (10) Slieve Gulion and Mourne Complexes. ODP are ocean drilling programme sites also labelled.

Cretaceous rocks, Triassic sandstones, and Moine Supergroup lithologies which had significant topographic relief at the time of lava eruption. Jurassic sediments also outcrop around limited parts of the perimeter of the island, although the extent of these lithologies underlying the flood basalts is unknown.

The Mull Lavas were divided into 3 main groups, originally identified by Bailey et al. (1924), correlated in detail and modified according to petrogenetic and geochemical characterisation by Kerr (1993, 1995a) and in subsequent publications. In chronological order, these groups are the Staffa Lava Group, Mull Plateau Group, the Coire Gorm type and the Central Mull Tholeiites. The Mull Plateau Group is the most complete lava succession on Mull and includes a series of predominantly alkali to transitional alkali Mg-rich basalts and hawaiites with minor mugearites and trachytes. Due to their earlier eruption and the

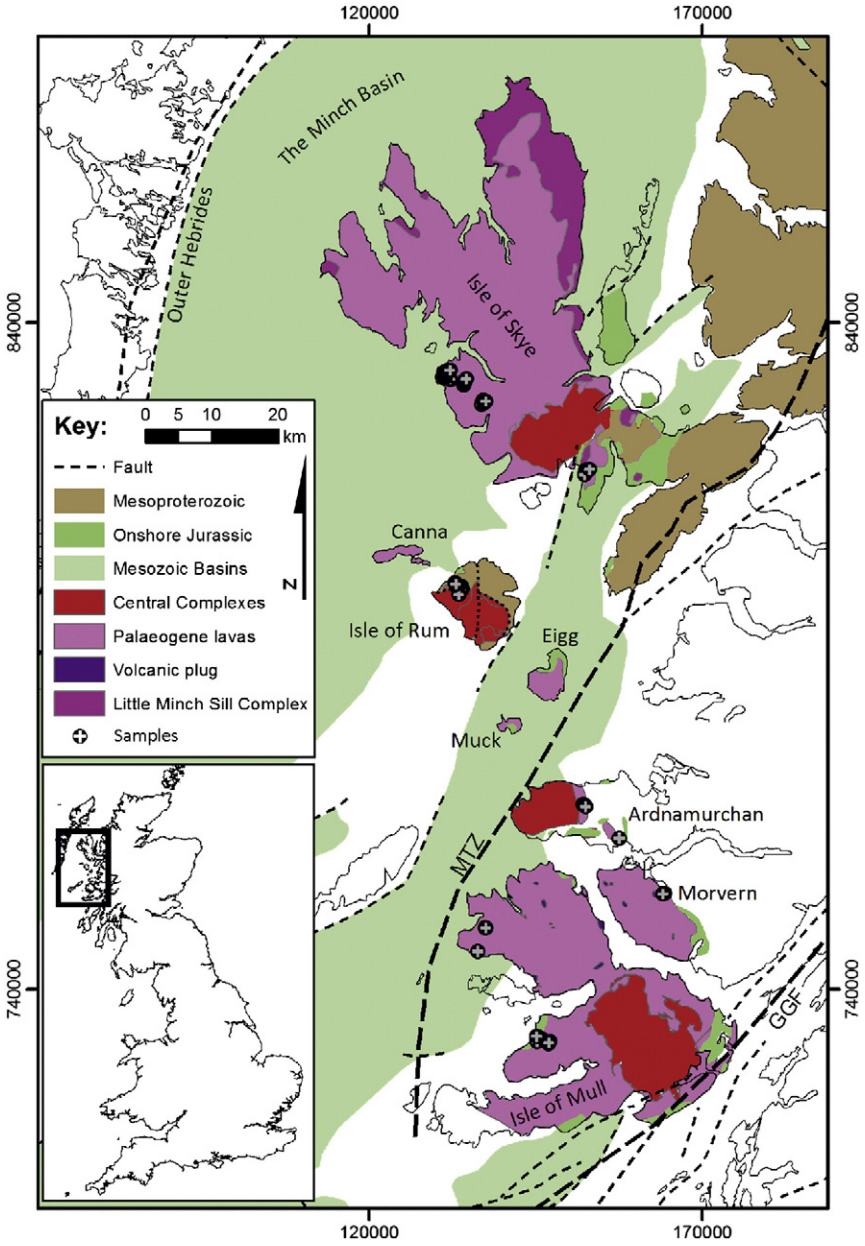

Fig. 2. Geology of the Hebridean portion of the BPIP and sedimentary rocks of the Torridonian and Hebrides Basin.

relatively high abundance of high-MgO lavas, all Mull and Morvern lava samples analysed during this study are from the Mull Plateau Group.

A series of elongate volcanic plugs are aligned in the direction of the regional dyke swarm and are found throughout Mull and Morvern. These plugs span a similar range of compositions including the Mull Plateau Group lavas and so are thought to have been shallow feeder conduits (Kerr, 1997). A range of tholeiitic dolerite plugs sampled by Kerr (1997) with varying MgO contents were selected for analysis during this study.

2.1.2. Lavas of the Ardnamurchan Peninsula

The Ardnamurchan Peninsula hosts three gabbroic intrusive centres, emplaced concentrically within country rocks of Moine psammites and pelites, Triassic and Jurassic sediments, and partially intruding into thin outliers of the Mull Lava Field (Bell and Williamson, 2002). A selection of these lavas from the lava field east of Beinn an Leathaid were analysed for PGE and Au in the present study.

2.1.3. The Small Isles lavas

Lavas of the Small Isles comprise predominantly olivine and tholeiitic basalts, with minor more evolved compositions (Emeleus and Bell, 2005). Lavas on the Isles of Canna and Sanday are at least 200 m thick, predominantly of alkali olivine basalt, hawaiite, and mugearite. Lavas of the Canna Lava Formation are preserved on NW Rum (Emeleus and Bell, 2005) and a series of samples from this area were analysed during this study (Fig. 3).

2.1.4. Isle of Skye lavas

The lava field on Skye (predominantly the 'Skype Main Lava Series'; 1.2–1.7 km thick transitional (tholeiitic–alkali) flood basalts) is mostly preserved to the NW of the Cuillin Central Complex (Fig. 3) and comprises alkali olivine basalts, hawaiites, mugearites, benmoreites, and trachytes (Thompson, 1982; Bell and Williamson, 2002). Lavas were extruded onto Mesoproterozoic Torridonian sediments of the

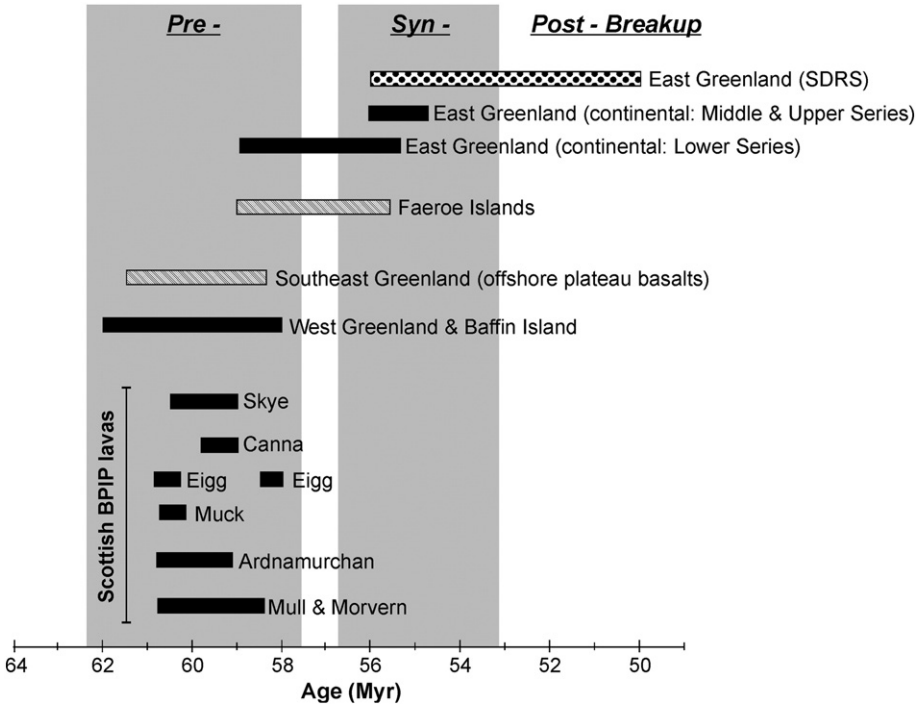

Fig. 3. Simplified timeline of lava sequences from phases 1 and 2 (pre- and syn-breakup; ca. 62–56 Ma) in the formation of the NAIP. See text for details (Chambers and Pringle, 2001 and references therein).

Torridon and Sleat Groups, Cretaceous and Jurassic sediments of the Mesozoic Hebrides Basin and parts of the Cuillin Central Complex. The absence of volcanic plugs associated with the lava fields on Skye and the more common observation of inter-lava sediments, may be an artefact of the relatively intermittent nature of Palaeogene volcanic activity in this area (Kerr, 1997). Bell and Williamson (2002), amongst others, have divided the Skye Main Lava Series into formations (10 to 760 m in thickness) and members based on flow lithological associations in each region of the island (north, north-central, west-central and south-central). However, extensive block faulting across the lava field, together with common inter-lava sedimentary units, makes full correlation across Skye difficult. All samples analysed during this study were sampled from the west-central and south-central sectors of the Skye Main Lava Series.

3. Analytical methods

Extensive major and trace element geochemical data and curated samples, exist for the Isle of Mull and Morvern basaltic lavas and doleritic plugs (Kerr, 1993, 1995a, b; Kerr et al., 1998, 1999). In this investigation, we analyse new samples along with a representative selection of curated BPIP lava and plug samples (Supplementary material Table A) for the PGE and Au.

Weathered material was removed from each sample before it was crushed to fine gravel. If present, amygdales and filled vesicles were hand-picked and removed from crushed samples before the remainder was milled to a fine powder in an agate planetary ball mill. Loss on Ignition (LOI) was determined gravimetrically by heating at 900 °C for two hours. Major and trace elements were measured by inductively coupled plasma optical emission spectrometry (ICP-OES) and inductively coupled plasma mass spectrometry (ICP-MS) respectively at Cardiff University following fusion using methods and instrumentation described by McDonald and Viljoen (2006). PGE and Au analysis was carried out by Ni-sulphide fire assay (sample weight 15 g) followed by Te co-precipitation and ICP-MS (Huber et al., 2001; McDonald and Viljoen, 2006). Accuracy for whole-rock elemental geochemistry was constrained by analysis of the certified international reference materials TDB1 and WMG1 for PGE and Au, and JB1a, NIM-P and NIM-N for all other trace and major elements (see Supplementary material Tables B and Ca–b). Precision for fire assay was estimated by repeat analysis of a sub-set of samples (Supplementary material Table D).

In total, 58 basalt lava samples (including 3 from Ardnamurchan, 1 from Rum, 40 from the Mull Plateau Group and 14 from the Skye Main Lava Series) and 11 dolerite plugs from Mull and Morvern were analysed by fire assay for PGE and Au during this study. All PGE and Au results are presented in Table 1. For major and trace element analyses 63 new lava samples were analysed from Skye, Rum and Ardnamurchan, along with 11 curated Mull dolerite plug samples. A full table of major and trace element data analysed during this study is available in Supplementary material Table E.

4. Geochemistry of NAIP and BPIP volcanics

Our results are compared with basaltic lavas collected and analysed for PGE by similar fire assay methods, from onshore Greenlandic plateau suites: West Greenland, Disko Island (Keays and Lightfoot, 2007); East Greenland, the Sortbre Profile in the Kangerlussuaq and Blosseville Kyst areas (Momme et al., 2002, 2006). Further comparison is made with PGE abundances in the seaward dipping reflector sequence offshore of Southeast Greenland (Philipp et al., 2001) and basaltic lavas from Iceland (Momme et al., 2003). Further Au data for Iceland and the Reykjanes Ridge was used for comparison (Webber et al., 2013).

4.1. Major elements

A selection of anhydrous major element variation diagrams (vs. MgO) for suites of lavas and plugs from the BPIP (Mull, Skye, Rum and Ardnamurchan) are shown in Fig. 4a–d. Data from Greenlandic lavas (onshore plateau basalts and offshore seaward dipping reflector sequences) and Icelandic lavas are also shown for comparison. These major element diagrams broadly define fractionation trends indicating fractionation of olivine and plagioclase, as has previously been detailed for these sequences (Kerr, 1995a; Fram and Lesher, 1997; Lightfoot et al., 1997; Saunders et al., 1998; Tegner et al., 1998a, b; Kerr et al.,

Table 1
Bulk rock PGE and Au results for BPIP lavas (in ppb).

Sample number	Location	Category	Rock type	Os (ppb)	Ir (ppb)	Ru (ppb)	Rh (ppb)	Pt (ppb)	Pd (ppb)	Au (ppb)	Mg#
AN_24	Arnamurchan	Lava	Basalt	0.04	0.06	0.16	0.06	0.44	0.16	0.11	37.43
AN_52	Arnamurchan	Lava	Basalt	0.17	0.24	1.00	0.41	3.98	1.59	0.11	67.00
AN_53	Arnamurchan	Lava	Basalt	0.11	0.11	0.25	0.14	2.12	0.73	0.21	65.74
AM10A(KJ)**	Isle of Mull	Lava	Basalt	0.10	0.08	0.17	0.08	4.13	2.98	0.81	67.74
AM10B(KJ)**	Isle of Mull	Lava	Basalt	0.16	0.08	0.11	0.09	6.17	2.66	0.71	67.77
AM10C(KJ)**	Isle of Mull	Lava	Basalt	0.07	0.07	0.11	0.14	5.69	2.22	0.62	66.57
AM7(KJ)**	Isle of Mull	Lava	Basalt	0.21	0.15	0.37	0.13	4.87	3.66	2.44	71.44
BB19(KJ)**	Isle of Mull	Lava	Basalt	0.03	0.05	0.12	0.23	2.02	1.77	0.40	51.93
BB20(KJ)**	Isle of Mull	Lava	Basalt	< d.t.	< d.t.	0.06	0.06	1.37	2.01	0.65	64.54
BB21(KJ)**	Isle of Mull	Lava	Basalt	0.31	0.26	0.44	0.15	9.20	2.80	0.78	70.10
BHI18(KJ)**	Isle of Mull	Lava	Basalt	0.15	0.06	0.18	0.08	4.49	2.99	0.58	68.16
BHI19(KJ)**	Isle of Mull	Lava	Basalt	0.79	0.36	0.73	0.25	7.78	4.52	0.52	73.47
BHI26(KJ)**	Isle of Mull	Lava	Basalt	0.07	0.08	0.17	0.14	1.61	1.71	0.23	68.64
BHI27(KJ)**	Isle of Mull	Lava	Basalt	0.21	0.11	0.15	0.08	3.49	1.95	0.84	66.95
BHI3(KJ)**	Isle of Mull	Lava	Basalt	0.04	0.07	0.11	0.07	5.45	2.22	0.98	68.34
BHI30(KJ)**	Isle of Mull	Lava	Basalt	0.81	0.79	1.47	0.43	7.49	7.42	0.78	73.03
BM10*	Isle of Mull	Lava	Basalt	1.00	0.90	1.47	0.38	4.63	1.65	1.01	79.29
BM12(KJ)**	Isle of Mull	Lava	Basalt	0.05	0.10	0.13	0.11	1.66	1.86	0.29	59.24
BM14(KJ)**	Isle of Mull	Lava	Basalt	0.53	0.51	0.64	0.31	7.41	4.03	0.56	67.58
BM15(KJ)**	Isle of Mull	Lava	Basalt	0.81	0.80	1.01	0.35	7.45	6.45	0.90	72.75
BM18*	Isle of Mull	Lava	Basalt	0.03	0.06	0.10	0.08	1.53	0.70	0.64	74.02
BM2*	Isle of Mull	Lava	Basalt	0.05	0.08	0.18	0.12	3.25	1.62	1.72	68.34
BM20*	Isle of Mull	Lava	Basalt	0.04	0.06	0.10	0.07	1.63	1.68	2.20	63.07
BM23*	Isle of Mull	Lava	Basalt	0.15	0.21	0.36	0.14	2.86	1.54	0.99	72.85
BM24*	Isle of Mull	Lava	Basalt	0.28	0.30	0.46	0.19	4.03	1.72	0.90	72.54
BM26*	Isle of Mull	Lava	Basalt	0.26	0.30	0.45	0.20	4.19	2.25	3.45	70.75
BM28*	Isle of Mull	Lava	Basalt	0.13	0.16	0.23	0.11	2.15	1.78	1.29	70.48
BM30*	Isle of Mull	Lava	Basalt	0.02	0.02	0.07	0.06	1.39	1.20	1.72	63.43
BM32*	Isle of Mull	Lava	Basalt	0.02	0.02	0.07	0.06	1.12	0.82	0.61	64.47
BM35*	Isle of Mull	Lava	Basalt	0.03	0.03	0.06	0.10	1.42	1.13	1.53	65.45
BM37*	Isle of Mull	Lava	Basalt	0.03	0.02	0.10	0.10	1.38	0.89	1.34	64.15
BM39*	Isle of Mull	Lava	Basalt	0.09	0.12	0.22	0.20	1.94	0.98	0.25	68.10
BM40*	Isle of Mull	Lava	Basalt	0.12	0.15	0.25	0.10	2.28	0.90	0.55	69.85
BM42*	Isle of Mull	Lava	Basalt	0.15	0.13	0.27	0.11	1.81	0.87	0.82	68.43
BM5(KJ)**	Isle of Mull	Lava	Basalt	0.14	0.10	0.21	0.10	3.50	4.97	0.35	67.33
BM6*	Isle of Mull	Lava	Basalt	0.18	0.16	0.32	0.15	4.06	1.99	2.19	64.31
BM6(KJ)**	Isle of Mull	Lava	Basalt	0.27	0.14	0.40	0.11	4.01	3.12	0.59	65.01
BM6A(KJ)**	Isle of Mull	Lava	Basalt	0.22	0.15	0.29	0.14	14.48	2.87	0.80	65.55
BM7(KJ)**	Isle of Mull	Lava	Basalt	0.38	0.37	0.71	0.28	5.12	5.26	1.12	73.22
BM8(KJ)**	Isle of Mull	Lava	Basalt	0.06	<d.t.	<d.t.	0.06	13.08	1.79	0.64	61.91
MR10(KJ)**	Isle of Mull	Lava	Basalt	0.36	0.40	0.60	0.19	4.42	2.98	13.02	72.69
MR11(KJ)**	Isle of Mull	Lava	Basalt	0.57	0.51	0.75	0.25	6.38	4.26	1.43	71.70
MR13(KJ)**	Isle of Mull	Lava	Basalt	0.24	0.32	0.45	0.18	5.76	3.81	1.20	70.47
RM_7	Isle of Rum	Lava	Basalt	0.12	0.09	0.19	0.22	2.01	2.57	0.52	57.92
SK_14	Isle of Skye	Lava	Basalt	0.14	0.36	0.69	0.41	1.40	1.52	1.57	42.64
SK_23	Isle of Skye	Lava	Basalt	0.03	0.23	0.42	0.48	3.16	1.39	0.79	46.33
SK_30	Isle of Skye	Lava	Hawaiite	0.04	0.09	0.16	0.09	0.65	0.54	0.09	62.08
SK_31	Isle of Skye	Lava	Basalt	0.05	0.09	0.46	0.27	9.36	1.36	0.30	61.42
SK_32	Isle of Skye	Lava	Basalt	0.05	0.05	0.11	0.10	0.65	0.27	0.08	66.14
SK_33	Isle of Skye	Lava	Hawaiite	0.04	0.07	0.35	0.18	1.24	1.17	0.24	39.92
SK_37	Isle of Skye	Lava	Mugearite	0.05	0.23	0.51	0.54	8.99	15.15	2.90	60.55
SK_38	Isle of Skye	Lava	Hawaiite	0.04	0.04	0.11	0.07	0.65	0.42	0.39	44.23
SK_41	Isle of Skye	Lava	Basalt	0.03	0.19	0.24	0.16	3.18	2.35	0.42	60.35
SK_42	Isle of Skye	Lava	Mugearite	0.11	0.16	0.22	0.17	0.86	0.64	0.18	69.01
SK_44	Isle of Skye	Lava	Basalt	0.23	0.48	0.66	0.35	2.91	2.78	0.34	68.92
SK_46	Isle of Skye	Lava	Hawaiite	0.06	0.06	0.14	0.14	0.63	0.45	0.17	63.69
SK_47	Isle of Skye	Lava	Picrobasalt	0.24	0.25	0.33	0.17	1.92	1.58	0.43	65.73
SK_66	Isle of Skye	Lava	Basalt	0.39	0.45	0.75	0.31	4.08	2.86	6.43	68.25
P10	Isle of Mull & Morvern	Plug	Dolerite	0.03	0.05	0.19	0.11	0.99	2.16	3.61	48.47
P11	Isle of Mull & Morvern	Plug	Dolerite	0.03	0.10	0.21	0.23	1.40	1.05	0.31	41.97
P21	Isle of Mull & Morvern	Plug	Dolerite	0.13	0.26	0.26	0.17	2.29	1.93	1.77	61.76
P27	Isle of Mull & Morvern	Plug	Dolerite	0.08	0.13	0.18	0.09	0.90	0.60	1.12	51.60
P28	Isle of Mull & Morvern	Plug	Dolerite	0.36	0.28	0.39	0.19	4.87	2.96	3.53	67.16
P29	Isle of Mull & Morvern	Plug	Dolerite	0.67	0.36	0.50	0.23	4.62	3.48	1.44	67.52
P30	Isle of Mull & Morvern	Plug	Dolerite	0.10	0.11	0.13	0.11	0.45	0.70	1.24	65.76
P34	Isle of Mull & Morvern	Plug	Dolerite	0.09	0.21	0.26	0.41	6.30	11.79	4.96	59.18
P55	Isle of Mull & Morvern	Plug	Dolerite	0.06	0.09	0.21	0.36	4.51	13.46	6.05	48.62
P6	Isle of Mull & Morvern	Plug	Dolerite	0.05	0.11	0.16	0.13	0.73	0.98	0.26	53.69
P9	Isle of Mull & Morvern	Plug	Dolerite	0.04	0.05	0.12	0.07	0.41	0.53	0.32	54.56
MORB	Atlantic Mid-Ocean Ridge		Bézos et al. (2005)		0.04	0.07		0.53	0.92		

Note that * indicates that major and trace elements were not analysed during this study but can be found in Kerr (1993). Similarly for samples marked as ** major and trace element data can be found in Jones (2005). Samples with code 'P' (Isle of Mull and Morvern plugs) were re-analysed for major and trace elements as part of this study (see Supplementary Table A) and the original analyses are available in Kerr (1997).

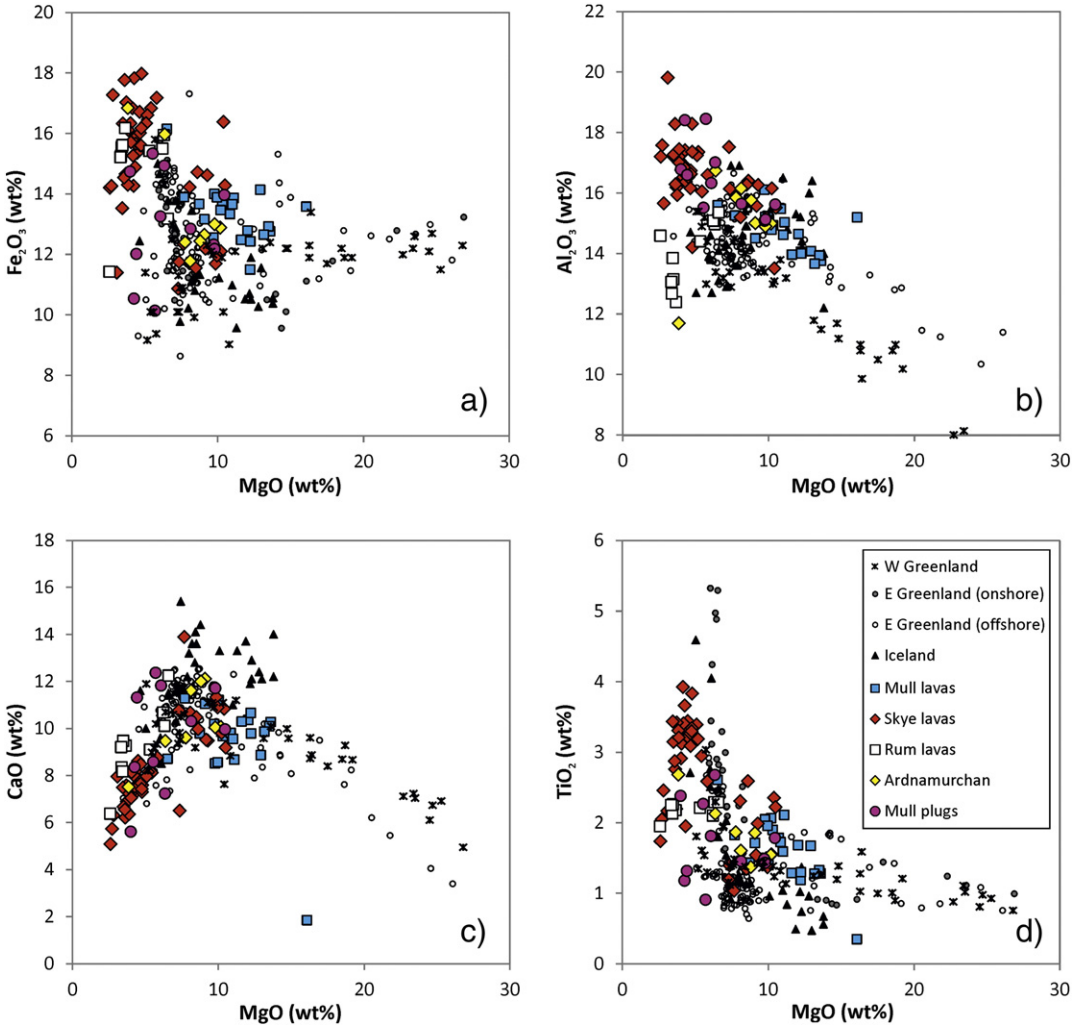

Fig. 4. Binary plots for major elements (anhydrous) vs. MgO (anhydrous) for BPIP lavas (this study; Kerr, 1993), and east Greenlandic, SDRS and Icelandic lavas (Lightfoot et al., 1997; Philipp et al., 2001 and references therein; Momme et al., 2002, 2003, 2006 and references therein).

1999; Philipp et al., 2001; Momme et al., 2003). Overall Fig. 4 demonstrates that the BPIP, Greenlandic and Icelandic volcanics are directly comparable in terms of lithological classification and major element composition.

4.2. Chalcophile elements

All chalcophile elements in Fig. 5a–d have been plotted relative to Mg# (i.e., [MgO]/([MgO] + [FeO])) as a proxy for magma fractionation.[1] High Mg# lavas have high Ni, Cr and Co concentrations, but some of the lowest Cu abundances. Overall Ni, Cr and Co concentrations in BPIP magmas (according to Mg#) overlap those of Greenlandic and Icelandic lavas. Some West Greenlandic lavas with high Mg# (>50) have anomalously low Ni concentrations (Fig. 5a). In contrast, Cu abundances in a significant number of BPIP lavas and plugs do not fully overlap other NAIP compositions (Fig. 5b), and some high-Mg# West Greenlandic lavas also have anomalously low Cu concentrations. All onshore East Greenlandic lavas follow an exponential negative trend of increasing Cu content with decreasing Mg#. The majority of offshore East Greenlandic lavas and Icelandic lavas follow a similar trend to onshore East Greenlandic lavas, although these are more scattered. However, the BPIP lavas and plugs appear to fall into one of two categories in Fig. 5b–a cluster that overlaps NAIP lavas for higher Mg# samples vs. a cluster that have lower Cu concentrations (either below this trend at higher Mg# or for samples with Mg# < 50). This division in BPIP samples does not fall rigorously within any one lava suite (e.g., Mull vs. Skye) although most Mull lavas overlap with NAIP.

4.3. Platinum-group elements and Au

Chondrite-normalised (McDonough and Sun, 1995) multi-element patterns for PGE and Au are shown in Fig. 6a–d for the BPIP lavas and plugs along with comparative patterns for Icelandic and Greenlandic lavas (Fig. 6e–h). It is clear that NAIP lava PGE abundances are typically elevated above MORB (Bézos et al., 2005)—see Table 1. Note that all BPIP lavas analysed for PGE and plotted in Fig. 6 onwards, are transitional alkali–tholeiitic and tholeiitic, to allow for a fair comparison with wider NAIP lavas available in the literature.

All NAIP samples have fractionated PGE such that Rh, Pt and Pd (Pd-group PGE; PPGE) are enriched relative to Os, Ir and Ru (Ir-group PGE; IPGE), but the relative PGE abundances in each sample suite vary considerably. With the exception of two Skye lava samples, chondrite-normalised Pd is similarly slight enriched over Pt in Fig. 6b. Lava samples from Mull fall into two categories—some have negative Pd anomalies relative to Pt, while the rest have nearly flat Pt to Pd normalised trends (Fig. 6c). Normalised Os and Ir concentrations in some Mull lavas exceed 0.001 × chondrite (0.48 ppb;

[1] Anhydrous FeO content was calculated from anhydrous Fe_2O_3 (total) analytical results according to the following conversion: $[(Fe_2O_3^{Total} - (TiO_2 + 1.5) / 1.1)]$ (Irvine, 1975).

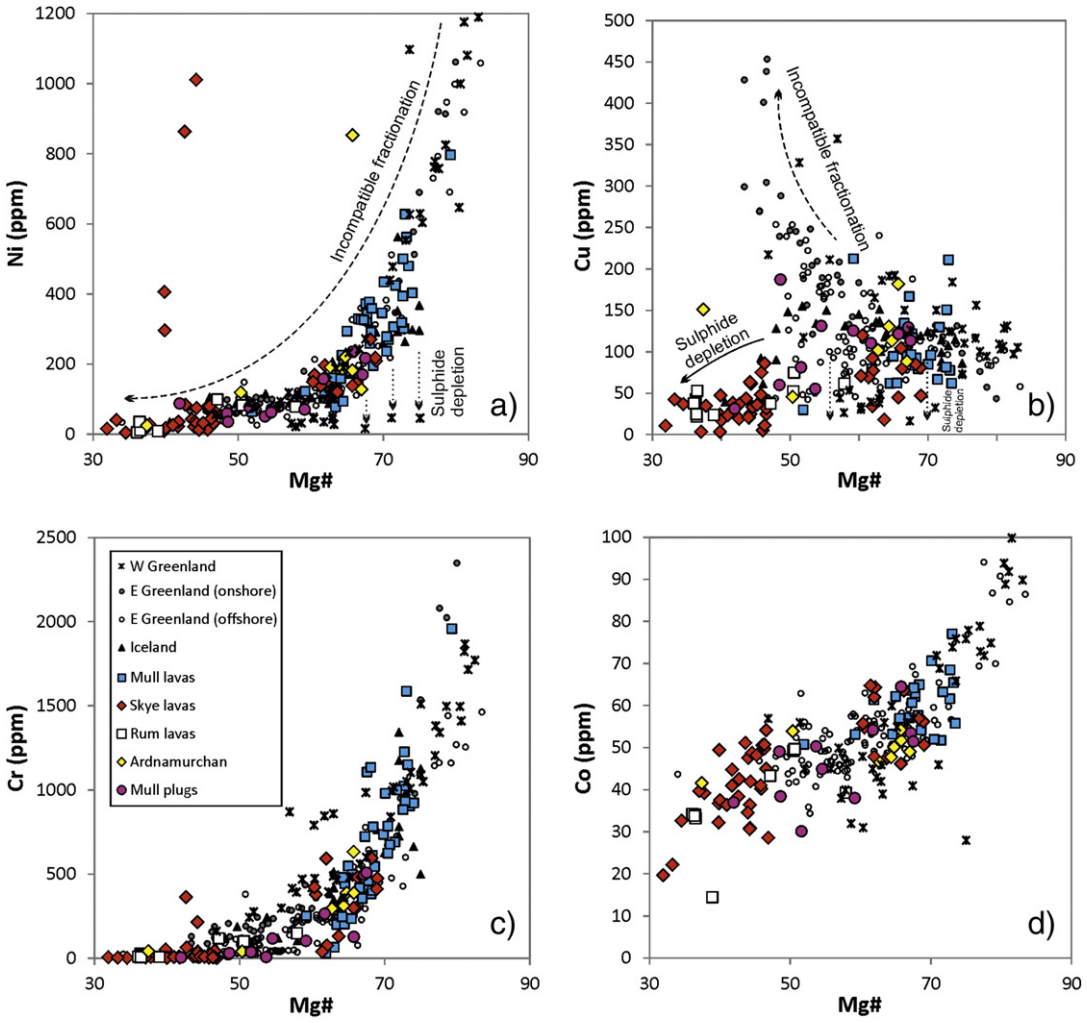

Fig. 5. Binary plots for chalcophile elements (anhydrous) vs. Mg#; (a) Ni, (b) Cu, (c) Cr, (d) Co. Symbols and data sources as in Fig. 4. Silicate fractionation and S-saturation trends indicated schematically in (c). See text for details of Mg# calculation. Note that dashed lines labelled 'crystal fractionation' are schematically shown and not calculated trends.

McDonough and Sun, 1995) whereas lavas from other areas fall consistently below this. In all BPIP lavas, normalised IPGE patterns are relatively flat (with $(Ru/Os)_N$ ranging 0.49 to 6.8), although there is variability in Os vs. Ir. For the BPIP lava samples, normalised Au content is highly variable—most lavas have slight positive Au anomalies (Fig. 6e). The normalised PGE patterns for the Mull doleritic plugs broadly overlap that of the Mull lavas, although the plugs lack any negative Pd anomalies and generally have higher Au. Overall, with the exception of Au, Pd and Pt, all BPIP lava compositions overlap Icelandic and Greenlandic (continental) lavas, although the systematic negative Ru anomaly of the Greenlandic ODP lavas (Fig. 6g) has not been found in any of BPIP samples.

The variation in PGE and Au abundances with Mg# are shown in Fig. 7a–f. For low Mg# (<65) BPIP samples, Ir and Ru concentrations are consistently low (<0.25 ppb for Ir, <0.5 ppb), but at Mg# > 65, Ir and Ru abundances sharply increase in line with existing data from Greenland. By contrast, Rh, Pt and Pd abundances are more variable and scattered when plotted relative to Mg# (Fig. 7c–e). In Fig. 7c–d, there is a broad positive correlation between increasing Mg# and increasing Rh and Pt concentrations, but this does not appear to be the case for Pd. Overall, BPIP lavas and plugs have lower absolute total PGE concentrations at Mg# > 50, in comparison to Greenlandic and Icelandic equivalents. Au abundances in BPIP and W Greenland samples are highly variable and do not correlate with Mg#, unlike the broad positive correlation for Icelandic lavas. However, there is no correlation for Icelandic–Reykjanes Ridge lavas (Fig. 7f).

We find no correlation between Pt/Pd ratio with Sm/Yb or Zr/Y (as proxies for mantle source region fertility—see Fig. 8a–b) nor with Dy/Yb (as a proxy for the presence of garnet in the mantle source region—Fig. 8c). There is also no correlation between Pt/Pd and Nb/La or Nb/Th (Fig. 8d–e) as proxies for crustal contamination across NAIP lavas.

Partitioning of PGE into sulphide liquid and silicate minerals can be identified by bivariant correlations between PGE and other chalcophile elements, as shown in Fig. 9a–d. For example, Ru is incompatible into olivine whereas Ir is weakly compatible (Capobianco et al., 1991; Brenan et al., 2002; Righter et al., 2004) and there is a positive correlation between in Ir and Ni in Fig. 9a. Rh and Ru have been experimentally shown to be compatible in Cr-spinel (e.g., Pagé et al., 2012 and references therein) and there is a positive correlation between Ru and Cr in Fig. 9b.

Pd and Cu have a positive correlation for most BPIP samples, although it is a broad correlation (Fig. 9c). By contrast, Greenlandic lavas are highly variable and scattered, and Icelandic lavas have a range of Pd concentrations but restricted Cu abundances. A very broad positive correlation is observed between Au and Pd (Fig. 9d). However, most BPIP lavas have lower Au abundances than Icelandic lavas. Cu and Pd are incompatible in silicate minerals but partition strongly into immiscible sulphide liquids formed during the S-saturation of silicate magmas. Estimates of partition coefficients range widely according to the experimental conditions (e.g., oxygen fugacity) used to establish them, and this is especially the case for PGE. In summary

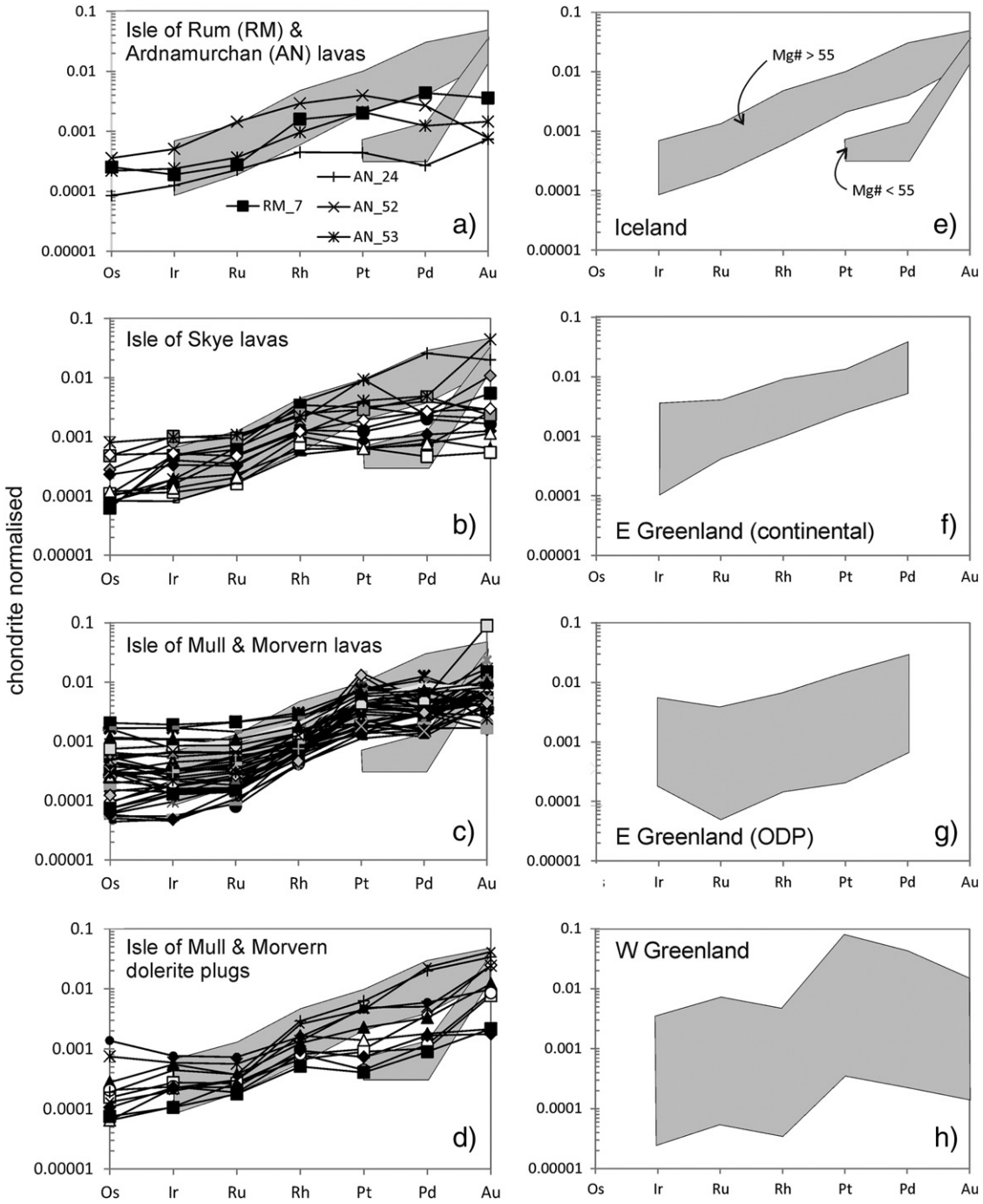

Fig. 6. Chondrite normalised (McDonough and Sun, 1995) PGE multi-element diagrams for BPIP lavas analysed during this study (a to d) and equivalent plots for Icelandic, east and west Greenlandic lavas (e to h) from Philipp et al. (2001), Momme et al. (2002, 2003), and Keays and Lightfoot (2007). Two distinct spidergram patterns are defined for Icelandic lavas, according to Mg# (e).

D_{Cu} ~ 1000 and D_{Pd} ~ 100,000 (Mungall and Brenan, 2014) but partitioning estimates for Pd can be particularly variable (57,000 to 580,000 in the experiments of Mungall and Brenan (2014) for example). Nonetheless, this order of magnitude difference for the partitioning behaviour of Cu in comparison to Pd allows ratio plots of these elements to identify S-saturation and sulphide depletion (as originally described by Barnes et al., 1993). If an immiscible sulphide liquid forms, both Cu and Pd will become concentrated in the sulphide and depleted in any residual silicate magma, but Pd will partition more strongly than Cu, sharply increasing the Cu/Pd ratio of the residual silicate magma. Hence if S-saturation was achieved at some prior stage of silicate magma fractionation, the Cu/Pd ratio of the silicate magma will be significantly elevated above primitive upper mantle (cf. Barnes et al., 1993).

The Cu/Pd ratio of BPIP lavas ranges 8000 to 1,000,000 and when plotted against Pd concentration these values overlap with East Greenlandic (offshore), West Greenlandic and Icelandic lavas (Fig. 10a). However, East Greenlandic (onshore) lavas form a tighter cluster of Cu/Pd ratios (~10,000 to 40,000). Although both elements are compatible into sulphide liquid, Pd partitions more strongly than Cu (Peach et al., 1990; Stone et al., 1990; Fleet et al., 1999; Mungall and Brenan, 2014 and references therein). Hence a sulphide accumulation trend vs. sulphide depletion magma trend is defined by Cu/Pd ratio. Lavas have been further subdivided according to Mg# in Fig. 9b–d.

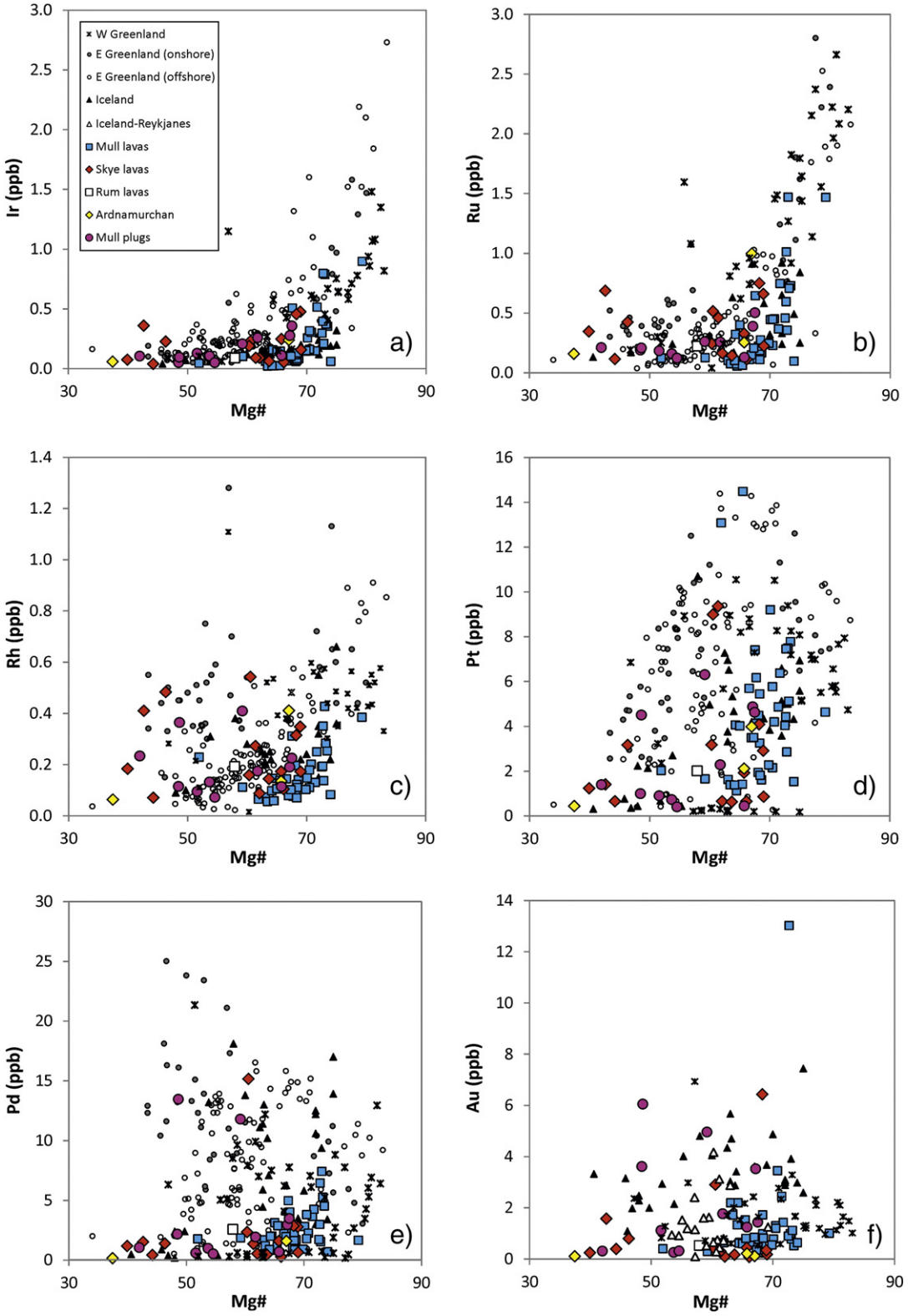

Fig. 7. Binary plots for PGE vs. Mg#; (a) Ir, (b) Ru, (c) Rh, (d) Pt, (e) Pd, (f) Au. Symbols and data sources as in previous figures and as well as Au data from Iceland–Reykjanes Ridge (Webber et al., 2013).

The clustered East Greenlandic (onshore) lavas with limited Cu/Pd ratio indicate that for this suite, S-saturation did not play a major role in changing chalcophile element concentration of ascending silicate magmas prior to eruption as lavas. Thus Cu/Pd ratio is 'unmodified' in East Greenlandic (onshore) lavas, irrespective of the degree of silicate magma fractionation. However, evidence of chalcophile element depletion can be identified in most BPIP samples (particularly for lavas with Mg# < 70) and West Greenlandic lavas, as well as some East Greenlandic (offshore seaward dipping reflector sequence) lavas. Additionally some East Greenlandic (offshore) and Icelandic lavas

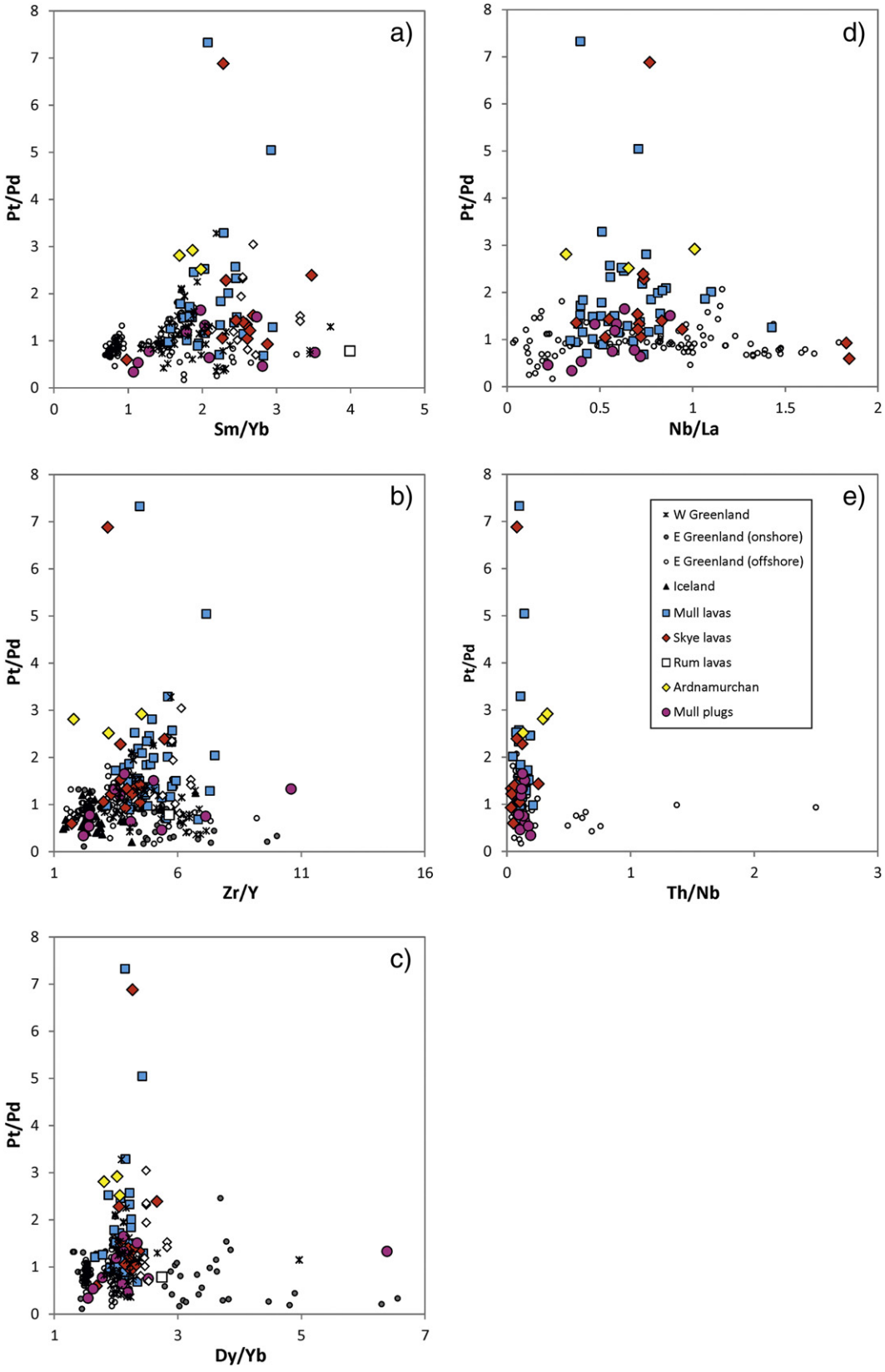

Fig. 8. Binary plots for Pt/Pd ratio vs. (a) Sm/Yb, (b) Zr/Y, (c) Dy/Yb, (d) Nb/La, (e) Th/Nb. Symbols and data sources as in previous figures.

have Cu/Pd ~ 6000 or within range of primitive mantle (McDonough and Sun, 1995)—see Fig. 9a–d.

Pd/Ir ratio can be used as a proxy for the degree of partial melting in the mantle source region of magmas (cf. Barnes and Lightfoot, 2005 and references therein), indicating whether melting has exhausted Cu-rich (PPGE-bearing) sulphides and begun to incorporate higher temperature IPGE-bearing MSS or metal alloys. During magma ascent through the crust, and if S-saturation is obtained

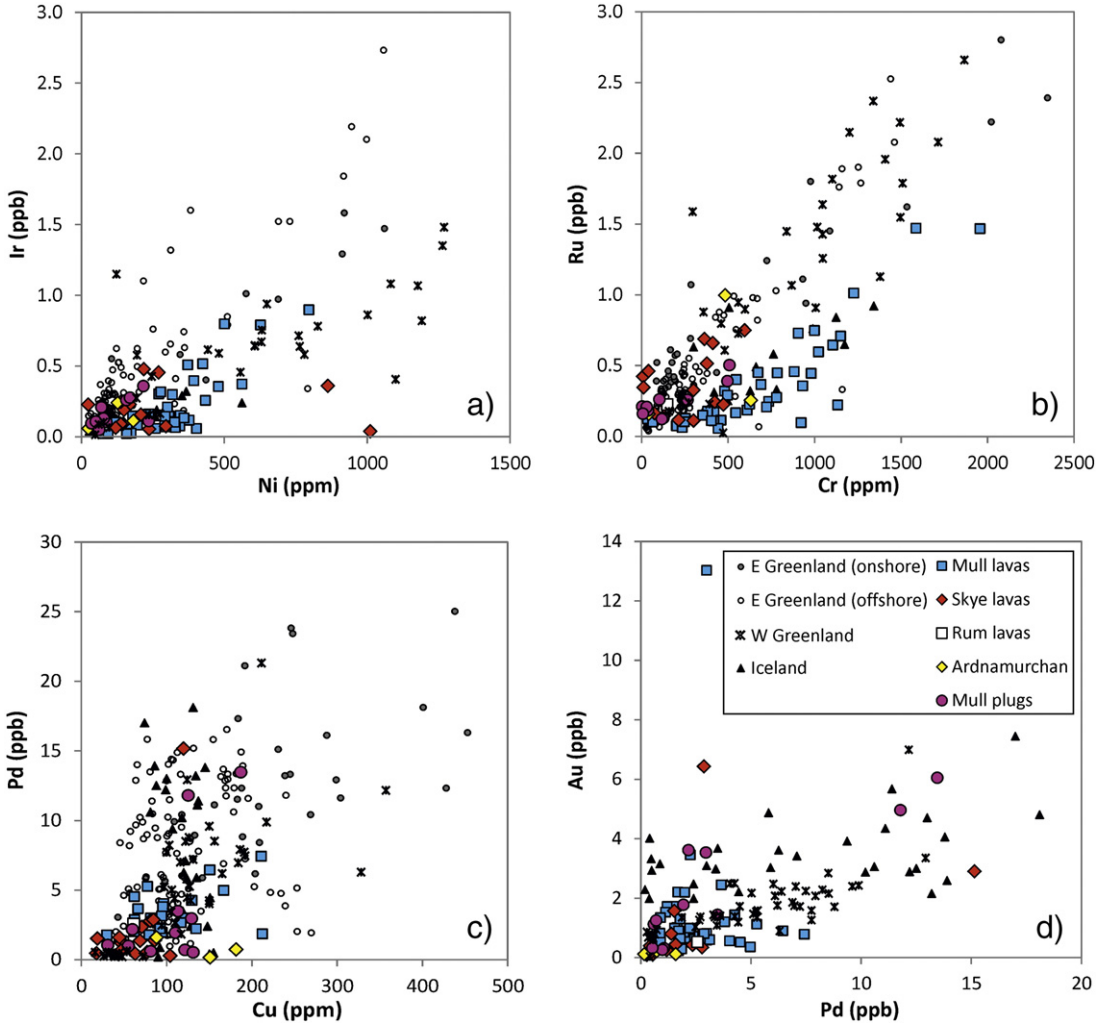

Fig. 9. Binary plots for PGE vs. chalcophile elements, paired according to partitioning behaviour; (a) Ir vs. Ni, (b) Ru vs. Cr, (c) Pd vs. Cu, (d) Au vs. Pd. Symbols and data sources as in previous figures.

(forming an immiscible sulphide liquid) the residual silicate magma will become depleted in both Pd and Ir alike, according to their strong partitioning into sulphide (D_{Ir} ~ 460,000; Mungall and Brenan, 2014 and references therein). Thus Pd/Ir ratios may remain broadly the same as prior to S-saturation, but absolute Pd and Ir concentrations will have decreased in the silicate magma. With very few exceptions, NAIP and BPIP samples have Pd/Ir ratios > primitive mantle (McDonough and Sun, 1995). However, BPIP samples do not overlap with the majority of other NAIP lavas, and sit at systematically lower Ir concentrations at equivalent Pd/Ir ratios (Fig. 11).

5. Discussion

The partitioning behaviour of chalcophile elements can be used as further evidence of fractional crystallisation throughout magma ascent, in a similar fashion to major elements. For example, the decrease in Ni with decreasing Mg# in Fig. 5a reflects incremental removal of Ni during olivine fractionation, although there are anomalously elevated Ni contents in four Skye lava samples and one Ardnamurchan lava, which do not fit this fractionation pattern. The anomalously low Ni concentrations in some high-Mg# West Greenlandic lavas suggest that Ni was depleted in these due to prior S-saturation. Hence sulphide depletion must have occurred early in the fractionation of these lavas (Fig. 5a). Co weakly partitions into olivine such that the positive correlation between Co and Mg# broadly fits olivine fractionation, although this is more scattered than for Ni. Cr partitions into spinel and hence the decrease in Cr abundance with decreasing Mg# reflects spinel fractionation. This is supported by the presence of negative Ru anomalies in Fig. 6a–d (BPIP) and 6 g (East Greenland) which suggest that chromite had crystallised earlier during silicate magma fractionation, and prior to S-saturation.

Cu is incompatible in silicate minerals so that as a silicate magma fractionates, the concentration of Cu in the remaining silicate magma increases sharply. As labelled in Fig. 5b, a significant proportion of BPIP lavas display low Cu concentrations (at lower Mg#) that does not fit with typical silicate fractionation, and instead indicates sulphide depletion during fractional crystallisation. If a silicate magma achieves S-saturation and exsolves an immiscible sulphide liquid, Cu partitions strongly into the sulphide ($D^{sul/sil}$ ~ 1000), leaving the remaining silicate magma (which ascends and erupts to form the lavas) depleted in Cu (e.g., Andersen et al., 2002). We identify this feature in most BPIP lavas with Mg# < 60, as well as minor Icelandic and East Greenlandic SDRS lavas. In addition some mafic lavas from Skye (Mg# 60–70) and West Greenland (Mg# 55–75) have anomalously low Cu contents and we suggest that these also signify S-saturation prior to eruption.

Various studies have shown that IPGE (such as Ir and Ru) are high-temperature PGE and mainly hosted by Fe-rich monosulphide solid solution (MSS) commonly included in silicate minerals in the mantle, or as refractory metal alloys of Os–Ir–Ru–Pt (Brenan and

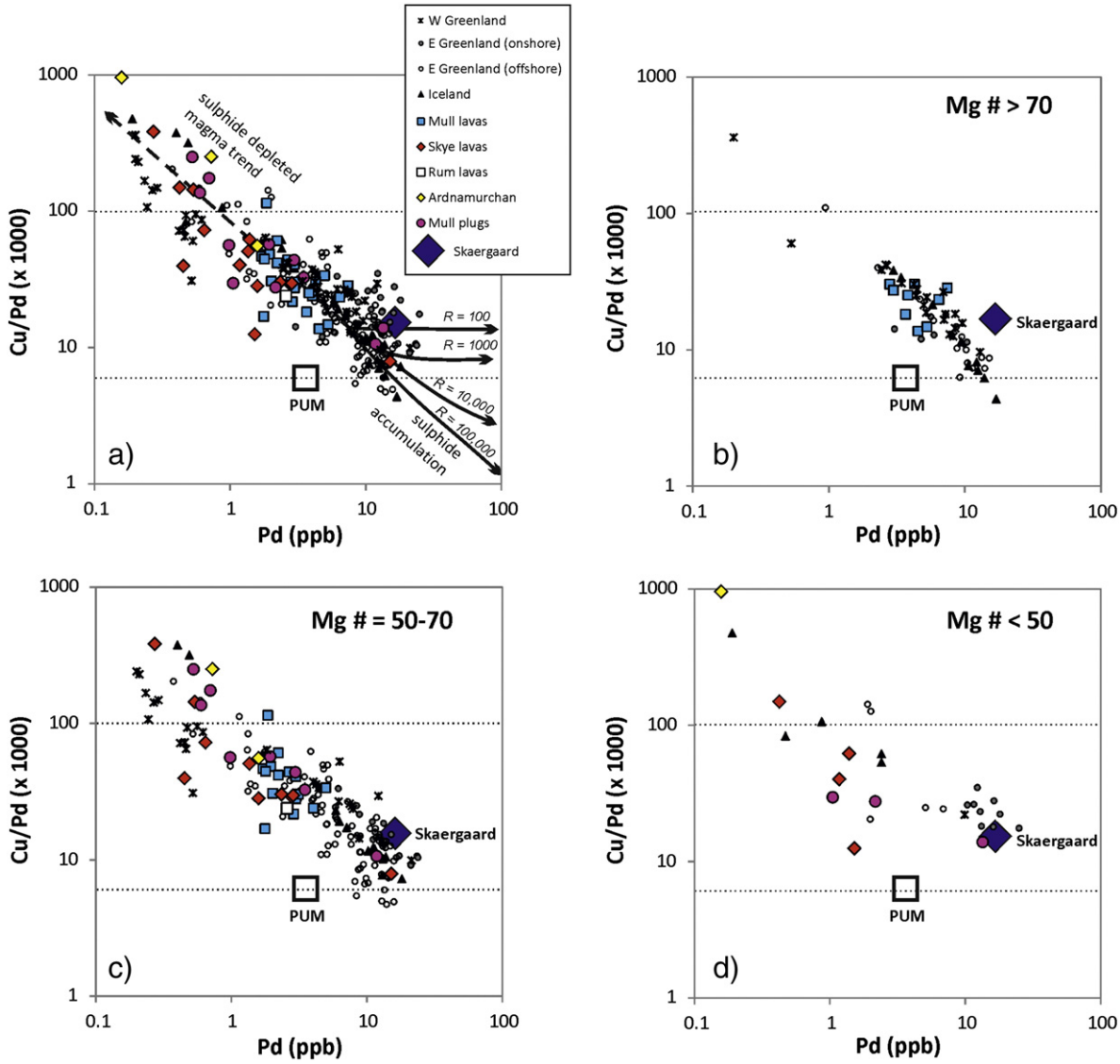

Fig. 10. PGE ratio plots. Cu/Pd vs. Pd according to Mg#; (a) all lavas, (b) lavas with Mg# > 70, (c) lavas with Mg# 50–70, (d) lavas with Mg# < 50. Primitive mantle from McDonough and Sun (1995). Sulphide depletion vector calculated from silicate/sulphide partition coefficients (Mungall and Brenan, 2014) for R factors (silicate/sulphide ratio) of 100 to 100,000. Skaergaard chilled composition (blue diamond) based on 265 ppm Cu (calculated by Thomassen and Nielsen, 2006) and 17 ppb Pd (chilled margin analysis by Vincent and Smales, 1956).

Andrews, 2001; Ahmed and Arai, 2002; Sattari et al., 2002; Bockrath et al., 2004b). By contrast PPGE (such as Pd) are predominantly hosted by interstitial Cu-rich mantle sulphides (Sattari et al., 2002; Bockrath et al., 2004a; Lorand et al., 2008). During mantle melting, PPGE are preferentially incorporated into magmas over IPGE (which are retained in unmelted monosulphide solution (MSS) and metal alloy residues), so that the initial Pd/Ir ratio is high and PGE spectra of magmas are positively fractionated (Keays, 1982; Barnes et al., 1988, 1990; McDonald et al., 1995; Maier and Barnes, 2004). With increasing degrees of partial melting, the Pd/Ir ratio of partial melts increases until mantle sulphides become exhausted in the source region (Naldrett, 2011). If partial melting exceeds this point of sulphide exhaustion, IPGE-bearing alloys enter the melt while Pd becomes diluted, thereby lowering the Pd/Ir ratio of the magma again. This effect is evident in Fig. 7a–b, where high Mg# numbers reflect a higher degree of mantle partial melting, enough to begin to significantly melt and incorporate IPGE (at Mg# > 65). Additionally some Greenlandic (offshore) and Icelandic lavas have Cu/Pd ~ 6000 (Fig. 10a) within range of primitive mantle (McDonough and Sun, 1995) and coupled with their high concentrations of Cu and Pd, this may suggest that sulphides were largely exhausted from the mantle source region during partial melting.

Palladium partitions very strongly into immiscible sulphide liquid and can be identified as being in solid solution within sulphide minerals, particularly pentlandite and pyrrhotite (e.g., Holwell et al., 2012 and references therein). The majority of BPIP samples have significantly lower Pd concentrations than wider NAIP lavas of equivalent Mg# (Fig. 7e) and this may be a reflection of a previous S-saturation event in BPIP lavas, such that residual silicate magmas which erupted as lavas were depleted in Pd during ascent. This feature can also be identified in some West Greenlandic lavas. Evidence of a systematic S-saturation event prior to BPIP lava eruption is also evident in Cu/Pd, particularly in lavas with Mg# < 70 (e.g., Fig. 10c). Pd/Ir vs. Ir (Fig. 11) shows a systematic offset between BPIP lavas and Greenlandic/Icelandic lavas, such that BPIP lavas have lower Ir concentrations at Pd/Ir ratios equivalent to Greenlandic/Icelandic lavas. As demonstrated by the model S-depletion arrows in Fig. 11, this suggests that BPIP lavas were strongly controlled by sulphide depletion prior to their eruption, whereas the majority of

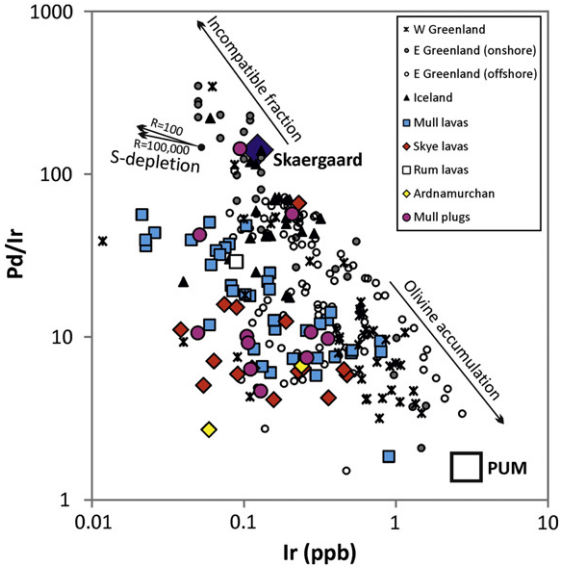

Fig. 11. Pd/Ir vs. Ir for all NAIP and BPIP lavas. Primitive mantle from McDonough and Sun (1995). Sulphide depletion vector calculated from silicate/sulphide partition coefficients (Mungall and Brenan, 2014) for R factors (silicate/sulphide ratio) of 100 to 100,000. Skaergaard chilled composition (blue diamond) based on 0.1 ppb Ir (estimated) and 17 ppb Pd (chilled margin analysis by Vincent and Smales, 1956).

Greenlandic and Icelandic lavas were controlled by silicate magma processes only (i.e., fractional crystallisation and olivine accumulation).

6. The S-saturation status for BPIP and NAIP lavas—regional mineralisation potential

The occurrence of S-saturation in a magma body may be assessed by the concentration of chalcophile elements within it (e.g., Andersen et al., 2002). Crustal contamination of magmas can trigger S-saturation, particularly if the country rocks contain significant amounts of S in the form of sulphides or sulphates (e.g., Li et al., 2002; Ripley et al., 2003; Naldrett, 2004, 2011; Keays and Lightfoot, 2009). During S-undersaturated fractional crystallisation of silicate magma, Cu concentration increases sharply in the residual melt, but if S-saturation is achieved, the immiscible sulphide liquid formed will strongly deplete the Cu content of the residual silicate magma (i.e., a sulphide depleted trend).

Trends relating to S-undersaturated fractional crystallisation and sulphide depletion have been identified in BPIP lava suites, including the two main lava series on Mull and Skye (see Fig. 5b). Some Mull lavas are S-undersaturated (e.g., Fig. 10b), whereas all Skye lavas have experienced S-saturation prior to eruption and follow a sulphide depletion magma trend (e.g., Fig. 10c). While Mull lavas generally have higher Mg# and are therefore less fractionated than Skye lavas, the fact that some Skye lavas with Mg# 60–70 also show anomalously low Cu concentrations is noteworthy. Both the Mull and Skye lava fields erupted through thick lower crustal sequences of Lewisian basement and Moine metasediments, with variable upper crustal sequences of Torridonian and Triassic rocks of the Hebrides Basin. However, current exposures on the Isle of Mull have only thin upper crustal S-rich Lower Jurassic sedimentary units (shales and mudrocks) on the periphery of the island, and it is uncertain how much of this material underlies the lava field. By contrast, a thick package of S-rich Jurassic sediments is prevalent on the Isle of Skye. Thus, we suggest that these Jurassic S-rich mudrocks were the main control on ascending BPIP magmas achieving S-saturation. This is a particularly relevant observation in the context of other NAIP settings.

The vast majority of offshore and onshore East Greenlandic lavas display S-undersaturated (i.e., silicate fractionation only) trends on Cu vs. Mg# plots (see Fig. 5b and Andersen et al., 2002). In the case of onshore East Greenlandic lavas, this is also supported by Cu/Pd ratio (Fig. 10). Although crustal sediments such as Cretaceous-Palaeocene marine shales, sandstones and marls (Soper et al., 1976; Larsen et al., 2001) are available for contamination on the East Greenlandic continental margin, there is a lesser volume of S-rich lithologies in comparison to the Scottish BPIP and Mesozoic Hebridean Basin. Icelandic lavas predominantly show an S-undersaturated trend, although some sulphide depletion is recorded in lavas with lower Mg#. Using Mg# as a proxy for fractional crystallisation (e.g., Fig. 10b–d where samples have been grouped according to Mg# categories), and in the absence of S sources from continental crust on Iceland, this limited S-saturation must be controlled by fractional crystallisation and/or magma mixing. It has been noted by Lightfoot et al. (1997) and Andersen et al. (2002) that lavas in West Greenland display geochemical features of both sulphide depletion and S-undersaturated silicate fractionation, and like the BPIP, different parts of these lava fields are dominated by flows that had undergone S-saturation prior to eruption.

The timing of S-saturation is critical in terms of PGE and metal enrichment in magmatic conduits underlying lava fields, and hence the potential for Norilsk–Talnakh style conduit-hosted orthomagmatic Ni–Cu–PGE mineralisation. Lavas near the base of the Vaigat Formation in West Greenland have the most marked crustal contamination signatures (based on lithophile element ratios and radiogenic isotope compositions — see Lightfoot et al., 1997 and Saunders et al., 1997 and references therein). However, because they were amongst the first lavas to be erupted in the province, Lightfoot et al. (1997) suggest that they had limited potential for magmatic mixing and within-conduit 'upgrading' of metal concentrations prior to eruption. This is supported by the observation of high-Mg# lavas with low chalcophile abundances (e.g., Ni depletion—Fig. 5a). With sustained magma flow through a conduit, sulphide liquid that ponds within that conduit can become enriched in chalcophile elements, possibly to economic levels, due to its continued interaction with fresh magma flushing through the conduit (e.g., Kerr and Leitch, 2005). But according to Lightfoot et al. (1997) and based on lava geochemistry, magmatic conduits or basal intrusions relating to lavas of the Vaigat Formation provide limited potential for significant high tenor orthomagmatic mineralisation. We suggest that this negates the 'recycling' of magmatic conduits (i.e., re-activation of conduits by later silicate magma batches represented by subsequent lavas) nor does it account for sustained magma flow through conduits, or the complexity of localised conditions such as variable crustal contamination. For example, the close-association, both spatially and temporally, of lavas fields in the BPIP shows that comparatively localised districts may have low vs. high S-contamination potential (for Mull and Skye respectively) and hence magmatic conduits underlying and feeding these lava fields may be similarly multifaceted. Therefore regional 'prospectivity', as determined by whether lavas experienced S-saturation or remained undersaturated, must take into account this variability.

In subsurface magmatic conduits, where sulphur has not degassed, S-isotopic studies ($\delta^{34}S$ and $\Delta^{33}S$) can identify the internal or external cause(s) for S-saturation. Hughes et al. (in press) assessed the whole-rock $\delta^{34}S$ signature of a suite of upper crustal narrow basaltic dykes and thick picritic sills intruded into Jurassic mudrocks on the Isle of Skye. These dykes have characteristically light $\delta^{34}S$ and are clearly contaminated with crustal S. Orthomagmatic sulphides with extremely light $\delta^{34}S$ occur deeper in the magmatic plumbing system in ultramafic volcanic plugs on the Isle of Rum (Power et al., 2003; Hughes et al., in press). Structural evidence discussed by Hughes et al. (under review) suggest that the vertical/subvertical volcanic plugs on Rum erupted through Jurassic sedimentary units, becoming strongly contaminated with isotopically light crustal S, inducing S-saturation and

forming an immiscible sulphide liquid which drained down through the partially crystallised conduit when activity ended (Hughes et al., under review).

Overall, the prevalence of fusible S-rich crustal rocks within the BPIP should be considered as a major exploration factor, both for the formation of immiscible sulphide liquids, but also for the collection or concentration of chalcophile elements including PGE in systems where magma input was sustained for long periods. The widespread identification of S contamination and saturation in upper crustal magmatic conduits (by $\delta^{34}S$) and lavas (by chalcophile element geochemistry) very clearly points to the presence of sulphides and enhanced mineralisation potential deeper within the Scottish BPIP magmatic plumbing system (as corroborated by Arndt, 2013) and therefore represent thus far unexplored exploration targets.

7. Pt/Pd ratio of NAIP magmas throughout continental break-up

Systematic differences in Pt and Pd abundance between lava suites across the NAIP are evident in Fig. 7d and e. BPIP lavas predominantly have lower Pd concentrations (at equivalent Mg#) in comparison to most Greenlandic and Icelandic lavas (Fig. 7e), and Pt vs. Mg# for BPIP lavas defines an entirely differently shaped trend to Greenlandic and Icelandic compositions, despite there being some overlap in the actual range of Pt (Fig. 7d). The sample preparation and analytical methodologies of our study for PGE in lavas are directly comparable to those of Philipp et al. (2001), Momme et al. (2002), Momme et al. (2003) and Keays and Lightfoot (2007). Therefore differences between Pd and Pt for the NAIP lava suites are unlikely to be due to analytical differences and appear to be true compositional features.

Plots of Pt vs. Pd (Fig. 12) for lavas from the NAIP are particularly instructive in assessing the compositional differences between the various areas. Lavas from the BPIP and West Greenland have Pt/Pd ratios near chondrite (1.9) and fall along a positive trend (statistically significant, $r^2 > 0.89$; Fig. 11a–b). At higher concentrations of either of these elements (i.e., >9 ppb Pt or Pd) more variability around a chondritic ratio is observed. Continental flood basalts from East Greenland (onshore) have extremely variable and scattered Pt/Pd ratios (Fig. 12c) but Pd is consistently enriched over Pt in comparison to BPIP and West Greenlandic lavas. East Greenlandic SDRS (offshore) lavas have a clear positive correlation ($r^2 > 0.88$) between Pt and Pd, but with a different sub-chondritic Pt/Pd ratio (Fig. 12d). Icelandic lavas also have a positive correlation between Pt and Pd ($r^2 > 0.90$) but with a much lower Pt/Pd ratio (Fig. 12e) than the offshore east Greenland lavas.

All the lava suites discussed in this study compare transitional alkalic–tholeiitic (e.g., BPIP) and tholeiitic (e.g., Iceland) picrites and basalts (with minor andesites). The differences in Pt/Pd ratio do not correspond either with a particular compositional series of lavas, nor with fractionation. Likewise, during magma ascent, S-saturation will not significantly fractionate Pt from Pd, as both elements have partition coefficients of a similar order of magnitude and will be partitioned correspondingly into an immiscible sulphide liquid. While in some crustal PGE-enriching environments (e.g., a long-lived conduit in which an immiscible sulphide liquid is progressively dissolved—Kerr and Leitch, 2005) Pt/Pd ratio may change, this effect is comparatively minor and would not be systematic across the various regions of the NAIP (cf. Fig. 12). In the NAIP Pt/Pd ratio appears to correspond to the age of the lava suites (i.e., the highest Pt/Pd ratio in the earliest lava suites of West Greenland and the BPIP vs. the lowest Pt/Pd in recent Icelandic lavas). The question arises whether this temporal change in the Pt/Pd ratio is indicative of a change in the plume-composition or geodynamic setting of the North Atlantic through time: from the initial eruption of picritic and basaltic magmas during early (proto-Iceland) mantle plume impingement, throughout continental rifting, the formation of oceanic lithosphere, and ultimately to the modern plume-oceanic rift setting of Iceland (Fig. 12f).

Possible causes for a systematic change in magma PGE geochemistry related to tectonic setting and/or geodynamic environment through time may include: (a) the degree or depth of partial melting; (b) changes in the mantle source region (i.e., enriched vs. depleted sources); (c) the melting regime and the shape of the melt column (i.e., cylindrical vs. triangular); (d) the mantle potential temperature; (e) the incorporation of deep mantle material in the plume; and/or (f) lithospheric contamination. Each of these possibilities is assessed below.

7.1. Degree of partial melting

Relative proportions of fertile mantle PGE concentrations are approximately chondritic (Carlson, 2005), although lower than chondrite in actual concentration by a factor of approximately 100–1000, as indicated by mantle-derived peridotite xenoliths (e.g., Luguet et al., 2003; Lorand et al., 2008; Maier et al., 2012 and references therein). During mantle melting, the first minerals to melt are sulphides, garnet and clinopyroxene, and so with increasing degrees of partial melting sulphides in the mantle source region become exhausted. However, the timing of sulphide exhaustion is primarily dependent the abundance of S in the mantle source, as well as whether an equilibrium batch melt, fractional melting, continuous melting, or dynamic melting model is assumed, and the shape and depth (pressure) of the melting profile (e.g., Rehkamper et al., 1999).

Partial melting of sulphide minerals in the mantle can be identified by fractionation of IPGE from PPGE, and therefore changes in Pd/Ir ratio (as previously outlined in Section 4.3). It is known from both experimental work and natural analogues of mantle materials that partial melting of base metal sulphides can produce Fe-rich MSS, Cu–Ni–Pd sulphide liquid with Fe-rich MSS and/or Ir–Pt alloys in the residue (e.g., Crocket, 2002; Luguet et al., 2003; Peregoedova et al., 2004). This will not only fractionate Pd from Ir, but could also fractionate Pd from Pt. We have already established that the range in Pd/Ir for each of the NAIP lava suites broadly overlaps despite lower absolute Ir concentrations due to PGE removal in sulphide liquids (Fig. 11). With the retention of Pt-bearing alloys in the mantle source region and/or entrainment and dissolution of Cu-rich (Pd-bearing) sulphide liquid into silicate magmas produced during partial melting, Pt and Pd may be fractionated from one another causing Pt/Pd ratios to vary according to the degree of partial melting. However, coupled with other melting proxies such as MgO content and Mg# (e.g., Figs. 4–5), a systematic change in Pt/Pd ratio related to the degree of mantle partial melting cannot be identified. Therefore this option is discounted as being a credible control on Pt/Pd ratio across the NAIP.

7.2. Melting source region and depth

Changes in asthenospheric mantle sources undergoing melting have previously been proposed for the NAIP. For example, Kerr (1993, 1995) and Kerr et al. (1999) used REE systematics to identify variations in partial melting of depleted (i.e., due to a prior melting event) vs. enriched asthenospheric mantle at both the spinel- and garnet-stability depths during the magmatism on the Isle of Mull. Similarly other incompatible trace elements in lavas and intrusive rocks have been used to constrain the depth and degree of melting in the BPIP (see Kent and Fitton, 2000 and references therein). Starkey et al. (2009) measured REE abundances in whole-rock lava samples and melt inclusions in olivine crystals from picritic lavas for Baffin Island and West Greenland, and identified both enriched and depleted mantle sources. Momme et al. (2006) used TiO_2 and REE contents to infer variations in melting depth and upper mantle sources for onshore East Greenlandic lavas. Isotopic studies by Kempton et al. (2000) and Murton et al. (2002) point to variations

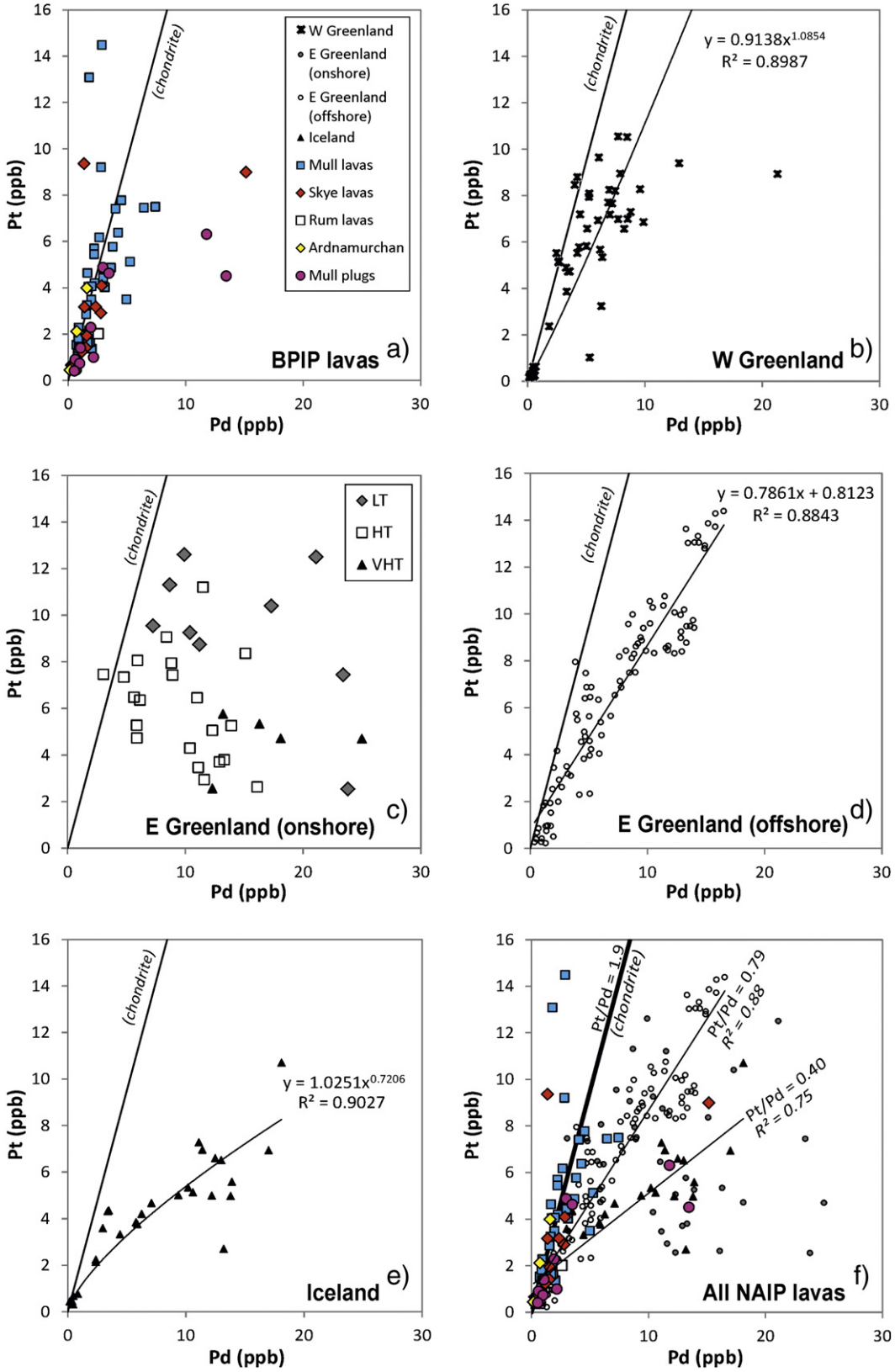

Fig. 12. Pt vs. Pd binary plots for lava suites from across the NAIP; (a) BPIP lavas, (b) West Greenlandic lavas (Disko Island; Keays and Lightfoot, 2007), (c) East Greenlandic lavas (Momme et al., 2002), (d) East Greenlandic SDRS lavas (Philipp et al., 2001), (e) Icelandic lavas (Momme et al., 2003), (f) all NAIP lavas. Chondritic ratio from McDonough and Sun (1995). Calculated trend lines and regressions labelled for plots (b), (d) and (e). Equivalent Pt/Pd ratios and trend line regressions labelled for each lava suite in (f).

in upper mantle components from up to 6 end members. However, although variations in melt sources of enriched vs. depleted end members and melting depths are clearly identifiable within the lava suites of the NAIP, this does not correlate with the broader temporal change in Pt/Pd observed across the NAIP as a whole (see Fig. 8a–c), which must reflect a more fundamental control.

7.3. Melting regime

Mantle melting modelling falls into two basic types; either simple batch melting or melt aggregates of near-fractional non-modal melting. In the case of the former, unreasonably high degrees of melting are required to explain the PGE content of Icelandic basalts, which cannot be reconciled with MgO content and other major and trace element systematics (Rehkamper et al., 1999). Therefore more recently, various non-modal melting models have been used to explain the combined lithophile and chalcophile element geochemistry of Icelandic and onshore East Greenlandic lavas (Momme et al., 2006). Non-modal melting models use either a triangular (analogous to spreading ridges; e.g., Momme et al., 2003) or a columnar (i.e., cylindrical; e.g., Keays, 1995; Rehkamper et al., 1999) melting regimes. For the East Greenlandic (onshore) lavas (Fig. 11c). Momme et al. (2006) suggested that lavas further inland with higher Ti contents were formed by a deeper triangular melting system in a continental rift setting, while lower Ti lavas nearer to the coast formed during continental rupture at greater degrees of shallower melting in a columnar melting regime. While these models reconcile the broad PGE (specifically Pd) and REE features of these East Greenlandic lavas, there is no correlation between Pt/Pd ratios of high- and low-Ti lavas. Both have highly scattered Pt/Pd (Fig. 11c) and so the melting regime and shape of the melt column are unlikely to exert a strong control on Pt/Pd across the NAIP.

7.4. Ambient temperature of melting or mantle potential temperature

Various estimates of mantle potential temperature exist for NAIP magmas. However, the methods by which temperatures are calculated include major and trace element thermodynamic modelling (e.g., Herzberg et al., 2007), estimates based on olivine compositions (e.g., Kent, 1995), and modelling based on geophysical constraints (e.g., seismic tomography, lithospheric uplift, buoyancy and/or estimates of active vs. passive upwelling; Brown and Lesher, 2014). All provide strong evidence for elevated mantle temperatures due to the presence of a mantle plume in this region. In particular Brown and Lesher (2014) calculate that the Palaeogene mantle was >125 °C hotter than ambient mantle temperature at the time, but suggest that this temperature elevation is comparatively muted beneath present-day Iceland (85–180 °C). Overall, the degree of uncertainty associated with mantle temperature estimates, coupled with the degree of uncertainty inherent in the use of differing methods of estimation, make a comparison of ambient mantle temperatures vs. Pt/Pd ratio difficult for the NAIP lava suites included in the current study. Nonetheless, the possibility that plume-related mantle potential temperatures have diminished during the formation of the NAIP and could systematically affect the Pt/Pd ratio is support by experimental studies that have shown that Pt-alloys have a significantly higher melting temperature than Pd-rich Cu sulphides or MSS (e.g., Peregoedova et al., 2004).

7.5. Incorporation of deep mantle or outer core material in the plume

Involvement of outer core material in mantle plumes could (in part) account for the elevated PGE, Ni and Fe contents observed in some plume-derived magmas, including those of the NAIP (e.g., Andersen et al., 2002). Andersen et al. (2002) calculated that PGE concentrations could be enriched 2.5 to 3 times above normal mantle contributions if as little as 0.5 to 1% of core material were contributed to a plume. Pt–Re–Os isotopic studies of plume-related magmas have widely documented an enriched $^{186}Os/^{187}Os$ signature, particularly noteworthy in lavas from West Greenland and Baffin Island, prompting suggestions that this represents incorporation of deep mantle or outer core–mantle boundary material in the plume magma (e.g., Pearson et al., 1999; Brandon and Walker, 2005). In addition, observations of elevated $^{3}He/^{4}He$ in the Icelandic plume and other plume settings (e.g., Kurz et al., 1983; Rison and Craig, 1983; Hilton et al., 2000 and references therein; Graham et al., 1998; Breddam et al., 2000), apparently provides further evidence of a deep mantle or core–mantle signature (e.g., Rison and Craig, 1983). However, more recent literature has highlighted the likelihood of elevated $^{3}He/^{4}He$ by decoupled entrainment, which implies that the He-isotopic signature cannot directly be used as evidence of core–mantle interaction (e.g., Starkey et al., 2009). Further doubt over the significance of elevated Re/Os, Pt/Os and $^{186}Os/^{187}Os$ signifying a core–mantle signature has come from W-isotopes in Hawaiian basalts, which only have bulk mantle compositions (Schersten et al., 2004; Carlson, 2005 and references therein).

Recent studies suggest that the initial volcanism in the BPIP and NAIP was unlikely to have contained a significant contribution from the outer core or from old recycled crustal material (Dale et al., 2009). Instead Os and He-isotopic studies suggest that early Baffin Island and West Greenlandic picrites were produced from a high percentage of melting in a depleted source region (leading to complete melting of mantle sulphides) at the head of the plume. Later phases of continental rifting and continued magmatism in modern Iceland contained a greater component of recycled oceanic crust melting (Dale et al., 2009). Kempton et al (2000) identified a higher contribution from a relatively enriched plume component in basalts from the SDRS offshore SE Greenland, than along the Reykjanes Ridge and Iceland today, and they suggest a diminishing plume component in the NAIP through time. Overall, if Dale et al. (2009) is accepted, then an outer core contribution to plume magmas cannot be the cause of Pt/Pd variation.

7.6. Lithospheric contamination

When assessing lithospheric contamination it is important to distinguish between crustal contamination and contamination from the subcontinental lithospheric mantle (SCLM). Deep crustal contamination of magmas by silicic basement is widely documented in lavas from across Greenland and the BPIP, using trace elements and isotopic compositions (see reviews in Saunders et al., 1997 and Kerr et al., 1999). However, the concentration of PGE within silicic crustal rocks is typically very low (see Carlson, 2005 and references therein) and they are therefore extremely unlikely to contribute to the PGE budgets of ascending mantle-derived magmas. There is no correlation between Pt/Pd and Nb/La (or other trace element proxies for contamination e.g., Ba/Nb, Nb/Th—see Fig. 8d–e) and so crustal contamination cannot be responsible for changing Pt/Pd ratio across NAIP lavas.

Pt/Pd ratios have previously been utilised to infer a metasomatic and 'on-craton' signature for various magmas, with an increased Pt/Pd ratio resulting from input of a metasomatic fluid-alteration component in the lithospheric mantle (Maier and Barnes, 2004). However, this does not reflect the physical nature of entrainment of PGE-bearing minerals and/or alloys affecting Pt/Pd ratio (alongside other PGE ratios), as originally proposed in the instance of kimberlites (McDonald et al., 1995). Nonetheless, metasomatic sulphides (with or without a demonstrable association of 'fluid'-rich alteration) are common in mantle peridotites and pyroxenites of the lithospheric mantle, as has been demonstrated in oceanic mantle, abyssal peridotites and alpine peridotites (e.g., Luguet et al., 2003; Alard et al., 2005; Luguet et al., 2008).

Hughes (2015) reports 3 distinctive populations of native base metal sulphides in the SCLM underlying northwest Scotland (Loch Roag, Isle of Lewis). One of these sulphide groups is systematically found in frozen melt pockets along grain boundaries (i.e., areas that would be most susceptible to melting). These sulphides have the highest abundance of PGE relative to the other sulphide groups in the xenolith, and include discrete micron-scale PtS (cooperite) platinum-group minerals. The bulk rock geochemistry of the Loch Roag peridotite xenoliths show chondritic Pt/Pd ratios, and chondrite-normalised PGE spectra show the xenoliths to be PPGE-rich with Pt and Pd at higher concentrations than that found in cratonic xenoliths from Western Greenland (Wittig et al., 2010) and 'primitive upper mantle' (McDonough and Sun, 1995; Palme and O'Neill, 2004). Although the age of these PtS-bearing

sulphides remains unquantified, based on a combination of whole-rock Re–Os isotope analyses and sulphide-specific Re/Os ratios, Hughes (2015) proposes that this group of sulphides are likely to be pre-Palaeogene, and could record a much older sulphide-bearing magmatic/metasomatic event.

Incorporation of fusible SCLM into plume magmas or ahead of a plume melting front has been suggested previously (e.g., Thompson and Morrison, 1988; Kerr, 1993; Saunders et al., 1997 and references therein; Foulger et al., 2005). This SCLM fusion is particularly feasible given the likelihood of lithospheric thinning or delamination inferred to take place during plume impingement on the base of continents in the North Atlantic (e.g., Kerr, 1994; Saunders et al., 1997). Hence the higher Pt/Pd ratio recorded in the older NAIP lava suites (e.g., BPIP and west Greenland) could reflect assimilation or mixing of ascending asthenospheric magmas with a (complex or multi-phase) Pt-rich lithospheric mantle end member. Given that sulphides are readily fusible and one of the first mineral phases to melt, we suggest that this SCLM interaction could have had a substantial effect on the precious metal budget of plume-derived asthenospheric magmas in the NAIP, essentially dictating the Pt/Pd ratio (>MORB) recorded spatially and temporally across the province.

Incorporation of PGE from the SCLM has previously been suggested for Pt-rich deposits such as the Bushveld Complex and Stillwater Complex (see Maier and Groves, 2011 and references therein). However, in these cases the involvement of SCLM in the PGE budget has been suggested by proxy, either by non-PGE geochemical evidence (e.g., elevated

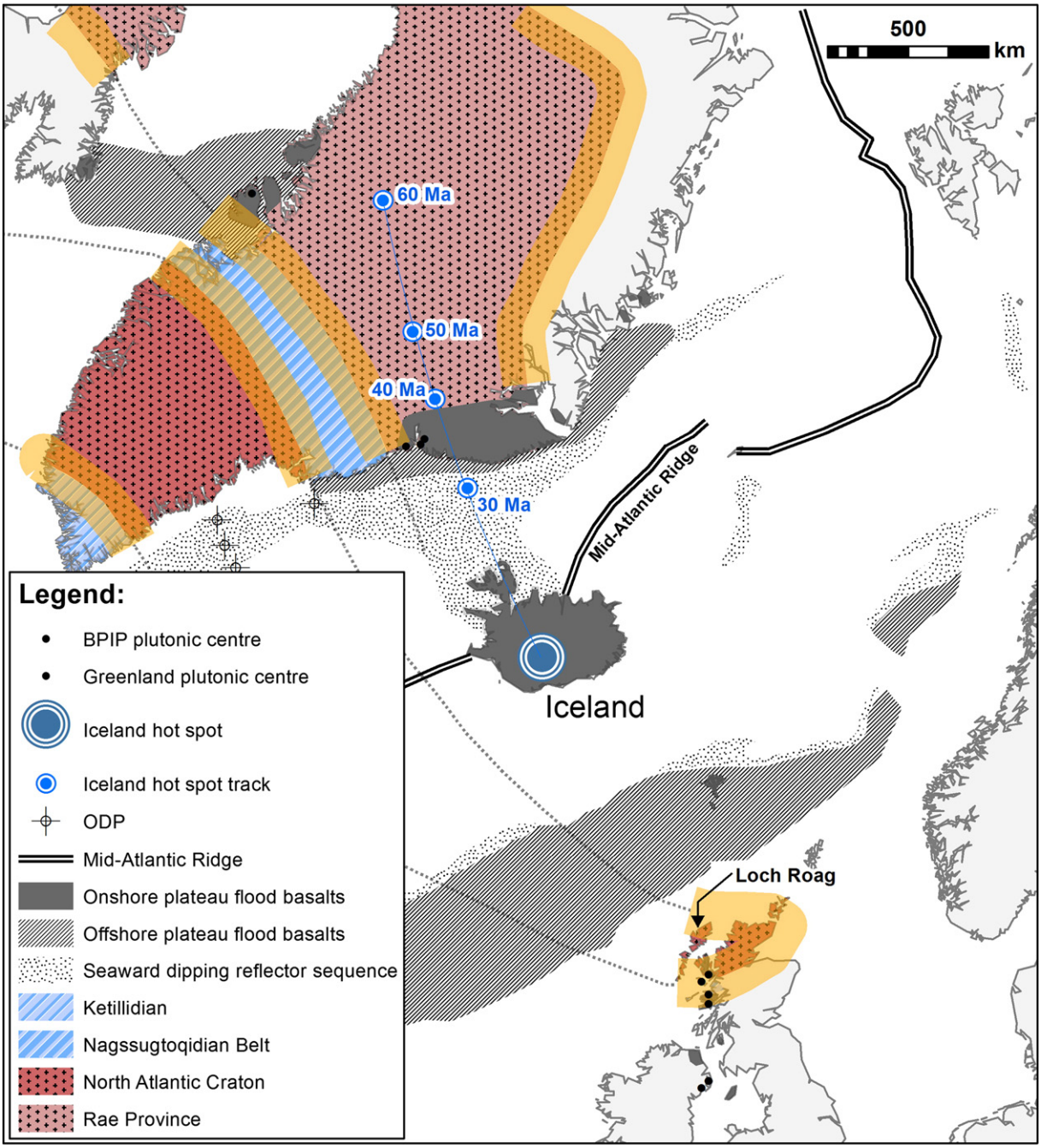

Fig. 13. Cratonic block reconstruction for the North Atlantic (based on Bleeker, 2003) vs. NAIP lava Pt/Pd ratio. Thick orange lines highlight cratonic margins (nominally to a width of 100–150 km, as a distance of <100 km was highlighted as being 'near craton margin' by Begg et al., 2010, and the Bushveld Complex sits approximately 130 km from the Kaapvaal cratonic margin).

lithophile element concentrations), or by radiogenic isotopes, and always in the absence of sulphide compositional analyses and petrography of SCLM material (i.e., mantle xenoliths) corresponding to that underlying such deposits. By contrast, between this study and Hughes (2015) we can clearly demonstrate that PGE-rich sulphides containing PtS (cooperite) exist in fusible lithologies (and along silicate grain boundaries) in parts of the Scottish SCLM and would have been available for contamination of asthenospheric plume magmas during the formation of the BPIP. While an ancient metasomatic process may ultimately have been responsible for the pre-enrichment of this cratonic SCLM by sulphide liquids, we suggest that such metasomatic enrichment was itself not coeval with the LIP magmatism responsible for PGE (especially Pt-rich) deposit formation (c.f., Barnes et al., 2010; Maier and Groves, 2011). Hence the dichotomy of whether SCLM- or plume-based melting is the dominant control on PGE prospectivity and relative Pt/Pd abundances, may obscure a deeper truth. Instead the preconditioning of cratonic SCLM may be an essential precursor to LIP magmatism in defining certain PGE deposit geochemical characteristics. This means that while the majority of magma is derived from asthenospheric mantle (possibly plume) source regions, during ascent precious metal ratios (e.g., Pt/Pd) may be modified by melting and contamination by multiple 'populations' of SCLM sulphides in specific petrographic settings (e.g., pre-existing and preserved melt pockets).

This raises the question—which regions of the SCLM are prone to this preconditioning, and why? For the NAIP lava suites underlain by ancient cratonic gneiss basement and SCLM, the higher Pt/Pd ratio in BPIP and West Greenlandic lavas at first appears to conflict with the more scattered Pt/Pd ratios of East Greenlandic (onshore) lavas. Craton reconstructions in the North Atlantic show that the NAC is bordered to the north by the Nagssugtoqidian orogenic belt (1900–1680 Ma; van Gool et al., 2002; Kolb, 2015) and that this Palaeoproterozoic mobile belt forms the southern border of the Rae Province—see Fig. 13. The Lewisian gneiss complex of Scotland, and the underlying SCLM (as represented by Loch Roag mantle xenoliths) occur on the very margin of the NAC, and are known to have undergone Palaeoproterozoic orogenesis (e.g., Loch Maree arc terranes c. 1900 Ma; Park, 2002). Lavas from West Greenland (Disko Island) also sit close to this mobile belt, although they actually overlie the southern margin of the Rae Province. By contrast NAIP lavas in East Greenland span the full width of the Rae Province and in particular lavas of the Sortebre Profile (analysed for PGE by Momme et al., 2002 and included in this study) are notably further from the Nagssugtoqidian orogenic belt than the West Greenlandic lavas.

Hence we suggest that depending on where the plume head impinges on the lithosphere, parts of the LIP may involve melting of SCLM regions that have experienced older metasomatism which introduced Pt-rich sulphides. This predisposition of Pt-enrichment is expected to be restricted along lithospheric mantle lineaments such as cratonic block boundaries and/or neighbouring orogenic belts (e.g., Nagssugtoqidian orogenic belt vs. NAC and Rae) and is not inherent in the depleted keel that makes up the majority of Archaean cratons themselves (e.g., Pearson et al., 2003). While the bulk rock Pt/Pd ratio of depleted cratonic keel mantle xenoliths may be broadly chondritic (e.g., Wittig et al., 2010) this does not inform us about PGE 'fusibility' which will be maximised when PGE-rich sulphides are developed along grain boundaries. In contrast, if the bulk rock PGE budget is strongly controlled by sulphides included within olivine or Cr-spinel, these are unlikely to contaminate passing asthenospheric magmas. Similarly, if sulphides along silicate grain boundaries only carry low PGE concentrations, their effect on asthenospheric magma PGE composition will also be negligible, despite their more feasible entrainment.

Lithospheric lineaments as conduits for ascending asthenospheric magmas and/or fluids have previously been highlighted as a control on the location of PGE mineralisation (e.g., Begg et al., 2010). We suggest that this is coupled with a fundamental geochemical control too, and that enrichment in precious metals along craton lineaments or margins is not a simple scenario. For example, we see no clear evidence to support a straightforward 'in-out box model' situation in which SCLM partial melting and S-depletion (thereby enriching PGE in the residual mantle sulphide) is followed by second-stage melting of the same SCLM (as proposed by Hamlyn and Keays, 1986). Instead the variety of sulphides reported widely in xenolith suites worldwide and from a range of tectonic settings (e.g., Guo et al., 1999; Lorand et al., 2004; Pearson et al., 2003 and references therein; Lorand et al., 2008; Delpech et al., 2012; Lorand et al., 2013) are testament to the true complexity of S-bearing events recorded in the lithospheric mantle. In the case of the BPIP and its relationship to the NAC, the multiple 'populations' of Loch Roag xenolith sulphides (Hughes, 2015) demonstrate the multi-stage enrichment that marginal cratonic lithospheric mantle, or cratonic block/boundary lineaments in the SCLM, may trace. The spatial relationship between ascending plume magmas and whether these magmas interact with pre-enriched (Pt-rich) cratonic boundaries or not, may exert a strong control over the Pt/Pd ratio of LIP magmas.

8. Conclusions

Analyses of the platinum-group element geochemistry of a series of lavas from the BPIP, in conjunction with other published studies of Greenlandic and Icelandic NAIP lavas, have enabled us to tackle two main themes pertaining to mineralisation potential and petrologic constraints on plume-SCLM magmatism and interaction.

1 The apparent enrichment (relative to MORB) in PGE abundances of the NAIP lavas and differing S-saturation controls across the region have been used to assess the mineralisation potential for orthomagmatic Ni–Cu–PGE sulphides in Greenland and Iceland. The widespread opportunity for crustal contamination to take place (particularly in the upper crust with widespread S-rich sediments of the Hebrides Basin) means that the BPIP represents one of the most fertile regions of the NAIP for Ni–Cu–PGE mineralisation.
2 Pt/Pd ratios change systematically across the NAIP, both spatially and temporally, such that the early NAIP lavas in West Greenland and the BPIP have the highest Pt/Pd ratios (approximately chondritic; 1.8). In comparison lavas erupted during the initiation of continental rifting and formation of oceanic crust have progressively lower Pt/Pd, such that modern Icelandic lavas are comparatively Pd-rich. This broad shift in Pt/Pd ratio coincides with changes in the geodynamic setting of the NAIP throughout its evolution — from the first formation of plume-derived magmas beneath thickened SCLM of the North Atlantic Craton and Rae Province, to modern oceanic rifting. Although this geochemical characteristic may be strictly plume controlled and therefore reflect a change in the dominance of the (proto-) Icelandic plume through time, the existence of pre-existing Pt-enriched SCLM underlying the margins of the NAC, and underlying early high Pt/Pd NAIP lavas suggests that there is a fundamental interaction between the plume and lithospheric mantle.
3 We suggest that Pt-enriched SCLM is restricted to the margins of cratons and along cratonic block lineaments such as Palaeoproterozoic inter-block mobile belts. We therefore favour a model whereby fusible sulphides in a fertile and Pt-rich marginal lithospheric keel become mobilised (via partial melting or wholesale lithospheric delamination) and incorporated into ascending asthenospheric magmas. The spatial relationship between intercratonic Proterozoic mobile belts and/or cratonic lineaments vs. the path of ascent of asthenospheric derived (plume) magmas dictates the PGE metal ratios inherent in LIP magmas and hence mineralisation within these provinces.

Supplementary data to this article can be found online at http://dx.doi.org/10.1016/j.lithos.2015.05.005.

Acknowledgements

HSRH acknowledges the financial support of the Natural Environment Research Council (NERC) for funding this work (studentship NE/J50029X/1) and open access publication. Anthony Naldrett and Kathryn Goodenough are thanked for their time and discussions. The authors thank two anonymous reviewers for their constructive and helpful feedback.

References

Ahmed, A.H., Arai, S., 2002. Unexpectedly high-PGE chromitite from the deeper mantle section of the northern Oman ophiolite and its tectonic implications. Contributions to Mineralogy and Petrology 143, 263–278.
Alard, O., Luguet, A., Pearson, N.J., Griffin, W.L., et al., 2005. In situ Os isotopes in abyssal peridotites bridge the isotopic gap between MORBs and their source mantle. Nature 436, 1005–1008.
Andersen, J.C.Ø., Rasmussen, H., Nielsen, T.F.D., Ronsbo, J.G., 1998. The Triple Group and the Platinova gold and palladium reefs in the Skaergaard Intrusion: stratigraphical and petrographic relations. Economic Geology 93, 488–509.
Andersen, J.C.Ø., Power, M.R., Momme, P., 2002. Platinum-group elements in the Palaeogene North Atlantic Igneous Province. In: Cabri, L.J. (Ed.), The Geology, Geochemistry, Mineralogy and Beneficiation of Platinum-Group Elements, pp. 1–30 (CIM Special Volume).
Arnason, J.G., Bird, D.K., 2000. A gold- and platinum-mineralized layer in gabbros of the Kap Edvard Holm Complex: field, petrologic, and geochemical relations. Economic Geology 95, 945–970.
Arndt, N.T., 2011. Insights into the geologic setting and origin of Ni–Cu–PGE sulfide deposits of the Norilsk–Talnakh region, Siberia. Reviews in Economic Geology 17, 190–215.
Arndt, N.T., 2013. The lithospheric mantle plays no active role in the formation of orthomagmatic ore deposits. Economic Geology 108, 1953–1970.
Bailey, E.B., Clough, C.T., Wright, W.B., Richey, J.E., et al., 1924. Tertiary and Post-Tertiary Geology of Mull. Loch Aline and Oban.
Barnes, S.-J., Lightfoot, P.C., 2005. Formation of magmatic nickel-sulfide ore deposits and processes affecting their copper and platinum-group element contents. In: Hedenquist, J.W., Thompson, J.F.H., Goldfarb, R.J., Richards, J.P. (Eds.), Economic Geology 100th Anniversary Volume, pp. 179–213.
Barnes, S.J., Boyd, R., Korneliussen, A., Nilsson, L.P., et al., 1988. The use of mantle normalization and metal ratios in discriminating between the effects of partial melting, crystal fractionation and sulphide segregation on platinum-group elements, gold, nickel and copper: examples from Norway. In: Prichard, H.M., Potts, P.J., Bowles, J.F.W., Cribb, S.J. (Eds.), Geo Platinum. Elsevier, London, pp. 113–143.
Barnes, S.J., Dunn, C.E., Curtin, G.C., Hall, G.E.M., 1990. The use of metal ratios in prospecting for platinum-group element deposits in mafic and ultramafic intrusions. Journal of Geochemical Exploration, pp. 91–99.
Barnes, S.-J., Couture, J.F., Sawyer, E.W., Bouchaib, C., 1993. Nickel–copper occurrences in the Belleterre–Angliers belt of the Pontiac Subprovince and the use of Cu–Pd ratios in interpreting platinum-group element distributions. Economic Geology 88, 1402–1419.
Barnes, S.J., Maier, W.D., Curl, E., 2010. Composition of the marginal rocks and sills of the Rustenburg Layered Suite, Bushveld Complex, South Africa: implications for the formation of the platinum-group element deposits. Economic Geology 105, 1491–1511.
Begg, G.C., Hronsky, J.A.M., Arndt, N.T., Griffin, W.L., O'reilly, S.Y., Hayward, N., 2010. Lithospheric, cratonic, and geodynamic setting of Ni-Cu-PGE sulfide deposits. Economic Geology 105, 1057–1070.
Bell, B.R., Williamson, I.T., 2002. Tertiary igneous activity. In: Trewin, N.H. (Ed.), 4th ed. The Geology of Scotland. The Geological Society, London, pp. 371–408.
Bézos, A., Lorand, J.P., Humler, E., Gros, M., 2005. Platinum-group element systematics in Mid-Oceanic Ridge basaltic glasses from the Pacific, Atlantic, and Indian Oceans. Geochimica et Cosmochimica Acta 69, 2613–2627.
Bird, D.K., Brooks, C.K., Gannicott, R.A., Turner, P.A., 1991. A gold-bearing horizon in the Skaergaard intrusion, East Greenland. Economic Geology 86, 1086–1092.
Bird, D.K., Arnason, J.G., Brandriss, M.E., Nevle, R.J., et al., 1995. A gold-bearing horizon in the Kap Edvard Holm Complex, East Greenland. Economic Geology 90, 1288–1300.
Bleeker, W., 2003. The late Archaean record: a puzzle in ca. 34 pieces. Lithos 71, 99–134.
Bockrath, C., Ballhaus, C., Holzheid, A., 2004a. Fractionation of the platinum-group elements during mantle melting. Science 305, 1951–1953.
Bockrath, C., Ballhaus, C., Holzheid, A., 2004b. Stabilities of laurite RuS_2 and monosulphide solid solution at magmatic temperatures. Chemical Geology 208, 265–271.
Brandon, A.D., Walker, R.J., 2005. The debate over core–mantle interaction. Earth and Planetary Science Letters 232, 211–225.
Breddam, K., Kurz, M.D., Storey, M., 2000. Mapping out the conduit of the Iceland mantle plume with helium isotopes. Earth and Planetary Science Letters 176, 45–55.
Brenan, J.M., Andrews, D., 2001. High-temperature stability of laurite and Ru–Os–Ir alloy and their role in PGE fractionation in mafic magmas. The Canadian Mineralogist 39, 341–360.
Brenan, J.M., Dalpe, C., McDonough, W.F., 2002. PGE's are Fractionated by Olivine–Melt Partitioning. Goldschmidt Conference Abstracts, Davos, Switzerland.
Brown, E.L., Lesher, C.E., 2014. North Atlantic magmatism controlled by temperature, mantle composition and buoyancy. Nature Geoscience 7, 820–824.
Capobianco, C.J., Drake, M.J., Rogers, P.S.Z., 1991. Crystal/melt partitioning of Ru, Rh and Pd for silicate and oxide phases. Lunar and Planetary Science 22, 179–180.
Carlson, R.W., 2005. Application of the Pt–Re–Os isotopic systems to mantle geochemistry and geochronology. Lithos 82, 249–272.
Chambers, L.M., Pringle, M.S., 2001. Age and duration of activity at the Isle of Mull Tertiary igneous centre, Scotland, and confirmation of the existence of subchrons during Anomaly 26r. Earth and Planetary Science Letters 193, 333–345.
Crocket, J.H., 2002. Platinum-group element geochemistry of mafic and ultramafic rocks. In: Cabri, L.J. (Ed.), The Geology, Geochemistry, Mineralogy and Mineral Beneficiation of Platinum-group Elements. Canadian Institute of Mining, Metallurgy and Petroleum, pp. 177–210.
Dale, C.W., Pearson, D.G., Starkey, N.A., Stuart, F.M., et al., 2009. Osmium isotopes in Baffin Island and West Greenland picrites: implications for the $^{187}Os/^{188}Os$ composition of the convecting mantle and the nature of high $^{3}He/^{4}He$ mantle. Earth and Planetary Science Letters 278, 267–277.
Delpech, G., Lorand, J.-P., Gregoire, M., Cottin, J.-Y., O'Reilly, S.Y., 2012. In-situ geochemistry of sulfides in highly metasomatized mantle xenoliths from Kerguelen, southern Indian Ocean. Lithos 154, 296–314.
Emeleus, C.H., Bell, B.R., 2005. British Regional Geology: The Palaeogene Volcanic Districts of Scotland. British Geological Survey, Nottingham.
Fleet, M.E., Crocket, J.H., Liu, M., Stone, W.E., 1999. Laboratory partitioning of platinum-group elements PGE/and gold with application to magmatic sulfide–PGE deposits. Lithos 47, 127–142.
Foulger, G.R., Natland, J.H., Anderson, D.L., 2005. A source for Icelandic magmas in remelted Iapetus crust. Journal of Volcanology and Geothermal Research 141, 23–44.
Fram, M.S., Lesher, C.E., 1997. Generation and polybaric differentiation of East Greenland Early Tertiary flood basalts. Journal of Petrology 38, 231–275.
Graham, D.W., Larsen, L.M., Hanan, B.B., Storey, M., et al., 1998. Helium isotope composition of the early Iceland mantle plume inferred from the Tertiary picrites of West Greenland. Earth and Planetary Science Letters 160, 241–255.
Groves, D.I., Bierlein, F.P., 2007. Geodynamic settings of mineral deposit systems. Journal of the Geological Society, London 164, 19–30.
Guo, J., Griffin, W.L., O'Reilly, S.Y., 1999. Geochemistry and origin of sulphide minerals in mantle xenoliths: Qilin, Southeastern China. Journal of Petrology 40, 1125–1149.
Hamlyn, P.R., Keays, R.R., 1986. Sulfur saturation and second-stage melts; application to the Bushveld platinum metal deposits. Economic Geology 81 (6), 1431–1445.
Herzberg, C., Asimow, P.D., Arndt, N., Niu, Y., et al., 2007. Temperatures in ambient mantle and plumes: constraints from basalts, picrites, and komatiites. Geochemistry, Geophysics, Geosystems 8 (n/a-n/a).
Hilton, D.J., Thirlwall, M.F., Taylor, R.N., Murton, B.J., et al., 2000. Controls on magmatic degassing along the Reykjanes Ridge with implications for the helium paradox. Earth and Planetary Science Letters 183, 43–50.
Holbrook, W.S., Larsen, H.C., Korenaga, J., Dahl-Jensen, T., et al., 2001. Mantle thermal structure and active upwelling during continental breakup in the North Atlantic. Earth and Planetary Science Letters 190, 251–266.
Holwell, D.A., Abraham-James, T., Keays, R.R., Boyce, A.J., 2012. The nature and genesis of marginal Cu–PGE–Au sulphide mineralisation in Paleogene Macrodykes of the Kangerlussuaq region, East Greenland. Mineralium Deposita 47, 3–21.
Huber, H., Koeberl, C., McDonald, I., Reimond, W.U., 2001. Geochemistry and petrology of Witwatersrand and Dwyka diamictites from South Africa: search for an extraterrestrial component. Geochimica et Cosmochimica Acta 65, 2007–2016.
Hughes, H.S.R., 2015. Temporal, Lithospheric and Magmatic Process Controls on Ni, Cu and Platinum-group Element (PGE) Mineralisation. PhD, Cardiff University.
Hughes, H.S.R., Boyce, A.J., McDonald, I., Davidheiser-Kroll, B., et al., 2015. Contrasting mechanisms for crustal sulfur contamination in the British Palaeogene Igneous Province: evidence from dyke and sill complexes on Skye. Journal of the Geological Society. http://dx.doi.org/10.1144/jgs2014-112 (in press).
Hughes, H.S.R., McDonald, I., Holwell, D.A., Boyce, A.J., et al., 2015w. Sulfide slumping in magma conduits: evidence from mafic–ultramafic plugs on Rum, North Atlantic Igneous Province. Journal of Petrology (under review).
Irvine, T.N., 1975. Crystallization sequences in the Muskox intrusion and other layered intrusions—II. Origin of chromitite layers and similar deposits of other magmatic ores. Geochimica et Cosmochimica Acta 39, 991–1020.
Jerram, D.A., Widdowson, M., 2005. The anatomy of Continental Flood Basalt Provinces: geological constraints on the processes and products of flood volcanism. Lithos 79, 385–405.
Jolley, D.W., Bell, B.R., 2002. The evolution of the North Atlantic Igneous Province and the opening of the NE Atlantic rift. In: Jolley, D.W., Bell, B.R. (Eds.), The North Atlantic Igneous Province: Stratigraphy, Tectonic, Volcanic and Magmatic Processes. The Geological Society, London, pp. 1–14.
Jones, K., 2005. The Laser Ablation ICP-MS Analysis of Olivine-hosted Melt Inclusions from the Plateau Group Lavas, Mull. PhD, Cardiff University, Scotland.
Keays, R.R., 1982. Palladium and iridium in komatiites and associated rocks: application to petrogenetic problems. In: Arndt, N.T., Nisbet, E.G. (Eds.), Komatiites. George Allen and Unwin, London, pp. 435–455.
Keays, R.R., 1995. The role of komatiitic and picritic magmatism and S-saturation in the formation of ore deposits. Lithos 34, 1–18.
Keays, R.R., Lightfoot, P.C., 2007. Siderophile and chalcophile metal variations in Tertiary picrites and basalts from West Greenland with implications for the sulphide saturation history of continental flood basalt magmas. Mineralium Deposita 42.
Keays, R.R., Lightfoot, P.C., 2009. Crustal sulfur is required to form magmatic Ni–Cu sulfide deposits: evidence from chalcophile element signatures of Siberian and Deccan Trap basalts. Mineralium Deposita 45, 241–257.
Kempton, P.D., Fitton, J.G., Saunders, A.D., Nowell, G.M., et al., 2000. The Iceland plume in space and time: a Sr–Nd–Pb–Hf study of the North Atlantic rifted margin. Earth and Planetary Science Letters 177, 255–271.

Kent, R.W., 1995. Magnesian basalts from the Hebrides, Scotland: chemical composition and relationship to the Iceland plume. Journal of the Geological Society 152, 979–983.
Kent, R.W., Fitton, J.G., 2000. Mantle sources and melting dynamics in the British Palaeogene Igneous Province. Journal of Petrology 41, 1023–1040.
Kerr, A.C., 1993. The Geochemistry and Petrogenesis of the Mull and Morvern Tertiary Lava Succession, Argyll. PhD, University of Durham, Scotland.
Kerr, A.C., 1994. Lithospheric thinning during the evolution of continental large igneous provinces: a case study from the North Atlantic Tertiary province. Geology 22, 1027–1030.
Kerr, A.C., 1995a. The geochemical stratigraphy, field relations and temporal variation of the Mull–Morvern Tertiary lava succession, NW Scotland. Transactions of the Royal Society of Edinburgh: Earth Sciences 86, 35–47.
Kerr, A.C., 1995b. The geochemistry of the Mull–Morvern lava succession, NW Scotland: an assessment of mantle sources during plume-related volcanism. Chemical Geology 122, 43–58.
Kerr, A.C., 1997. The geochemistry and significance of plugs intruding the Tertiary Mull–Morvern lava succession, western Scotland. Scottish Journal of Geology 33, 157–167.
Kerr, A., Leitch, A.M., 2005. Self-destructive sulfide segregation systems and the formation of high-grade magmatic ore deposits. Economic Geology 100, 311–332.
Kerr, A.C., Kent, R.W., Bell, B.R., Jolley, D., 1998. Discussion on application of palynological data to the chronology of the Palaeogene lava fields of the British Province. Journal of the Geological Society, London 155, 733–735.
Kerr, A.C., Kent, W.R., Thomson, B.A., Seedhouse, J.K., et al., 1999. Geochemical evolution of the Tertiary Mull volcano, Western Scotland. Journal of Petrology 40, 873–908.
Kolb, J., 2015. Structure of the Palaeoproterozoic Nagssugtoqidian Orogen, South-East Greenland: model for the tectonic evolution. Precambrian Research 255, 809–822.
Kurz, M.D., Jenkins, W.J., Hart, S.R., Clague, D., 1983. Helium isotopic variations in volcanic rocks from Loihi Seamount and the Island of Hawaii. Earth and Planetary Science Letters 66, 388–406.
Larsen, M., Bjerager, M., Nedkvitne, T., Olaussen, S., Preuss, T., 2001. Geological Survey of Greenland Bulletin 189, 99–106.
Lawver, L.A., Muller, R.D., 1994. Iceland hotspot track. Geology 22, 311–314.
Li, C., Ripley, E.M., Maier, W.D., Gomwe, T.E.S., 2002. Olivine and sulfur isotopic compositions of the Uitkomst Ni–Cu sulfide ore-bearing complex, South Africa: evidence for sulfur contamination and multiple magma emplacements. Chemical Geology 188, 149–159.
Lightfoot, P.C., Hawkesworth, C.J., Olshefsky, K., 1997. Geochemistry of Tertiary tholeiites and picrites from Qeqertarssuaq (Disko Island) and Nuussuaw, West Greenland with implications for the mineral potential of comagmatic intrusions. Contributions to Mineralogy and Petrology 128, 139–163.
Lorand, J.-P., Delpech, G., Gregoire, M., Moine, B., O'Reilly, S.Y., Cottin, J.-Y., 2004. Platinum-group elements and the multistage metasomatic history of Kerguelen lithospheric mantle (South Indian Ocean). Chemical Geology 208, 195–215.
Lorand, J.-P., Luguet, A., Alard, O., Bezos, A., et al., 2008. Abundance and distribution of platinum-group elements in orogenic lherzolites; a case study in a Fontete Rouge lherzolite (French Pyrénées). Chemical Geology 248, 174–194.
Lorand, J.-P., Luguet, A., Alard, O., 2013. Platinum-group element systematics and petrogenetic processing of the continental upper mantle: a review. Lithos 164–167, 2–21.
Luguet, A., Lorand, J.-P., Seyler, M., 2003. Sulfide petrology and highly siderophile element geochemistry of abyssal peridotites: a coupled study of samples from the Kane Fracture Zone (45°W 23°20 N, MARK area, Atlantic Ocean). Geochimica et Cosmochimica Acta 67, 1553–1570.
Luguet, A., Pearson, D.G., Nowell, G.M., Dreher, S.T., Coggon, J.A., Spetsius, Z.V., Parman, S.W., 2008. Enriched Pt-Re-Os isotope systematics in plume lavas explained by metasomatic sulfides. Science 319 (5862), 453–456.
Maier, W.D., Barnes, S.-J., 2004. Pt/Pd and Pd/Ir ratios in mantle-derived magmas: a possible role for mantle metasomatism. South African Journal of Geology 107, 333–340.
Maier, W.D., Groves, D.I., 2011. Temporal and spatial controls on the formation of magmatic PGE and Ni–Cu deposits. Mineralium Deposita 46, 841–857.
Maier, W.D., Peltonen, P., McDonald, I., Barnes, S.J., et al., 2012. The concentration of platinum-group elements and gold in southern African and Karelian kimberlite-hosted mantle xenoliths: implications for the noble metal content of the Earth's mantle. Chemical Geology 302–303, 119–135.
McDonald, I., Viljoen, K.S., 2006. Platinum-group element geochemistry of mantle eclogites: a reconnaissance study of xenoliths from the Orapa kimberlite, Botswana. Applied Earth Science 115, 81–93.
McDonald, I., De Wit, M., Smith, C.B., Bizzi, L.A., et al., 1995. The geochemistry of the platinum-group elements in Brazilian and southern African kimberlites. Geochimica et Cosmochimica Acta 59, 2883–2903.
McDonough, W.F., Sun, S., 1995. The composition of the earth. Chemical Geology 120, 223–253.
Momme, P., Tegner, C., Brooks, K., Keays, R., 2002. The behaviour of platinum-group elements in basalts from the East Greenland rifted margin. Contributions to Mineralogy and Petrology 143, 133–153.
Momme, P., Óskarsson, N., Keays, R.R., 2003. Platinum-group elements in the Icelandic rift system: melting processes and mantle sources beneath Iceland. Chemical Geology 196, 209–234.
Momme, P., Tegner, C., Brooks, C.K., Keays, R.R., 2006. Two melting regimes during Paleogene flood basalt generation in East Greenland: combined REE and PGE modelling. Contributions to Mineralogy and Petrology 151, 88–100.
Mungall, J.E., Brenan, J.M., 2014. Partitioning of platinum-group elements and Au between sulfide liquid and basalt and the origins of mantle–crust fractionation of the chalcophile elements. Geochimica et Cosmochimica Acta 125, 265–289.
Murton, B.J., Taylor, R.N., Thirlwall, M.F., 2002. Plume-ridge interaction: a geochemical perspective from the Reykjanes Ridge. Journal of Petrology 43, 1987–2012.
Naldrett, A.J., 2004. Magmatic Sulphide Deposits: Geology, Geochemistry and Exploration. Springer, Berlin.
Naldrett, A.J., 2011. Fundamentals of magmatic sulfide deposits. In: Li, C., Ripley, E.M. (Eds.), Society of Economic Geologists, Reviews in Economic Geology. Magmatic Ni–Cu and PGE Deposits: Geology, Geochemistry, and Genesis vol. 17, pp. 1–51.
Pagé, P., Barnes, S.-J., Bédard, J.H., Zientek, M.L., 2012. In situ determination of Os, Ir, and Ru in chromites formed from komatiite, tholeiite and boninite magmas: implications for chromite control of Os, Ir and Ru during partial melting and crystal fractionation. Chemical Geology 302–303, 3–15.
Palme, H., O'neill, H.S.C., 2004. Cosmochemical estimates of mantle composition. Treatise on Geochemistry 2, 1–38.
Park, R.G., 2002. The Scourie Dyke Suite. Geological Society Memoirs. 26. The Geological Society, London, pp. 21–28.
Peach, C.L., Mathez, E.A., Keays, R.R., 1990. Sulfide melt–silicate melt distribution coefficients for noble metals and other chalcophile elements as deduced from MORB: implications for partial melting. Geochimica et Cosmochimica Acta 54, 3379–3389.
Pearson, D.G., Larsen, L.M., Walker, R.J., Woodland, S.J., et al., 1999. The deep sources of plumes: phenium–osmium platinum–osmium isotopic and platinum-group element systematics of high helium-3/helium-4 West Greenland picrites. Proceedings of the 9th Annual Goldshmidt Conference 223.
Pearson, D.G., Canil, D., Shirey, S.B., 2003. Mantle samples included in volcanic rocks: xenoliths and diamonds. Treatise on geochemistry 2, 171–275.
Peregoedova, A., Barnes, S.-J., Baker, D.R., 2004. The formation of Pt–Ir alloys and Cu–Pd-rich sulfide melts by partial desulfurization of Fe–Ni–Cu sulfides: results of experiments and implications for natural systems. Chemical Geology 208, 247–264.
Philipp, H., Eckhardt, J.-D., Puchelt, H., 2001. Platinum-group elements (PGE) in basalts of the seaward-dipping reflector sequence, SE Greenland Coast. Journal of Petrology 42, 407–432.
Power, M.R., Pirrie, D., Andersen, J.C.Ø., 2003. Diversity of platinum-group element mineralization styles in the North Atlantic Igneous Province: new evidence from Rum, UK. Geological Magazine 140, 499–512.
Rehkamper, M., Halliday, A.N., Fitton, J.G., Lee, D.-C., et al., 1999. Ir, Ru, Pt, and Pd in basalts and komatiites: new constraints for the geochemical behavior of the platinum-group elements in the mantle. Geochimica et Cosmochimica Acta 63, 3915–3934.
Righter, K., Campbell, A.J., Humayun, M., Hervig, R.L., 2004. Partitioning of Ru, Rh, Pd, Re, Ir, and Au between Cr-bearing spinel, olivine, pyroxene and silicate melts. Geochimica et Cosmochimica Acta 68, 867–880.
Ripley, E.M., Lightfoot, P.C., Li, C., Elswick, E.R., 2003. Sulfur isotopic studies of continental flood basalts in the Noril'sk region: implications for the association between lavas and ore-bearing intrusions. Geochimica et Cosmochimica Acta 67, 2805–2817.
Rison, W., Craig, H., 1983. Helium isotopes and mantle volatiles in Loihi Seamount and Hawaiian Island basalts and xenoliths. Earth and Planetary Science Letters 66, 407–426.
Roest, W.R., Srivistava, S.P., 1989. Sea-floor spreading in the Labrador Sea: a new reconstruction. Geology 17, 1000–1003.
Sattari, P., Brenan, J.M., Horn, I., McDonough, W.F., 2002. Experimental constraints on the sulfide- and chromite–silicate melt partitioning behavior of rhenium and the platinum-group elements. Economic Geology 97, 385–398.
Saunders, A.D., Fitton, J.G., Kerr, A.C., Norry, M.J., et al., 1997. The North Atlantic Igneous Province. In: Mahoney, J.J., Coffin, M.F. (Eds.), Large Igneous Provinces: Continental, Oceanic, and Planetary Flood Volcanism. American Geophysical Union, Washington DC, pp. 45–93.
Saunders, A.D., Larsen, H.C., Fitton, J.G., 1998. Magmatic development of the southeast Greenland Margin and evolution of the Iceland plume: geochemical constraints from Leg 152. Proceedings of the Ocean Drilling Program, Scientific Results 152, pp. 479–501.
Schersten, A., Elliott, T., Hawkesworth, C.J., Norman, M., 2004. Tungsten isotope evidence that mantle plumes contain no contribution from the Earth's core. Nature 427, 234–237.
Single, R.T., Jerram, D.A., 2004. The 3D facies architecture of flood basalt provinces and their internal heterogeneity: examples from the Palaeogene Skye Lava Field. Journal of the Geological Society, London 161, 911–926.
Sinton, C.W., Hitchen, K., Duncan, R.A., 1998. $^{40}Ar/^{39}Ar$ geochronology of silicic and basic volcanic rocks on the margins of the North Atlantic. Geological Magazine 135, 161–170.
Soper, N.J., Higgins, A.C., Downie, C., Matthews, D.W., Brown, P.E., 1976. Late Cretaceous-early Tertiary stratigraphy of the Kangerdlugssuaq area, East Greenland, and the age of opening of the northeast Atlantic. Journal of the Geological Society of London 132, 85–104.
Starkey, N.A., Stuart, F.M., Ellam, R.M., Fitton, J.G., et al., 2009. Helium isotopes in early Iceland plume picrites: constraints on the composition of high 3He/4He mantle. Earth and Planetary Science Letters 277, 91–100.
Stone, W.E., Crocket, J.H., Fleet, M.E., 1990. Partitioning of palladium, iridium, platinum, and gold between sulfide liquid and basalt melt at 1200 °C. Geochimica et Cosmochimica Acta 54, 2341–2344.
Storey, M., Duncan, R.A., Tegner, C., 2007. Timing and duration of volcanism in the North Atlantic Igneous Province: implications for geodynamics and links to the Iceland hotspot. Chemical Geology 241, 264–281.
Tegner, C., Duncan, R.A., Bernstein, S., Brooks, C.K., et al., 1998a. $^{40}Ar/^{39}Ar$ geochronology of Tertiary mafic intrusions along the East Greenland rifted margin: relation to flood basalts and the Iceland hotspot track. Earth and Planetary Science Letters 156, 75–88.
Tegner, C., Lesher, C.E., Larsen, L.M., Watt, W.S., 1998b. Evidence from the rare-earth-element record of mantle melting for cooling of the Tertiary Iceland plume. Nature 395, 591–594.
Thomassen, B., Nielsen, T.F.D., 2006. The Mineral Potential of the East Greenland Palaeogene Intrusions. In: Secher, K. (Ed.), Geological Survey of Denmark and Greenland.

Thompson, R.N., 1982. Magmatism of the British Tertiary Volcanic Province. Scottish Journal of Geology 18, 49–107.
Thompson, R.N., Morrison, M.A., 1988. Asthenospheric and lower-lithospheric mantle contributions to continental extensional magmatism: an example from the British Tertiary Province. Chemical Geology 68, 1–15.
van Gool, J.A.M., Connelly, J.N., Marker, M., Mengel, F.C., 2002. The Nagssugtoqidian Orogen of West Greenland: tectonic evolution and regional correlations from a West Greenland perspective. Canadian Journal of Earth Sciences 39 (5), 665–686.
Vincent, E.A., Smales, A.A., 1956. The determination of palladium and gold in igneous rocks by radioactivation analysis. Geochimica et Cosmochimica Acta 9, 154–160.
Webber, A.P., Roberts, S., Taylor, R.N., Pitcairn, I.K., 2013. Golden plumes: substantial gold enrichment of oceanic crust during ridge–plume interaction. Geology 41, 87–90.
White, N., Lovell, B., 1997. Measuring the pulse of a plume with the sedimentary record. Nature 387, 888–891.
White, R., McKenzie, D., 1989. Magmatism at rift zones: the generation of volcanic continental margins and flood basalts. Journal of Geophysical Research 94, 7685.
Wittig, N., Webb, M., Pearson, D.G., Dale, C.W., Ottley, C.J., Hutchison, M., Jensen, S.M., Luguet, A., 2010. Formation of the North Atlantic Craton: Timing and mechanisms constrained from Re–Os isotope and PGE data of peridotite xenoliths from S.W. Greenland. Chemical Geology 276, 166–187.